Appendix H
LIQUEFACTION EFFECTS AND ASSOCIATED HAZARDS

H.1 PURPOSE AND SCOPE

In support of the NCHRP 12-49 effort to develop the next generation of seismic design provisions for new bridges, a study of the effects of liquefaction and the associated hazards of lateral spreading and flow, was undertaken. This Appendix presents a summary of the results of that study (NCHRP 12-49 Liquefaction Study).

The motivation for the study was the recommended change in the design return period for ground motions for a rare or "Maximum Considered Earthquake" (MCE) used in the recommended provisions. The recommended provisions are based on using ground motions for the MCE that correspond to a probability of exceedence of 3 percent in 75 years (2,475-year return period) for most of the United States. In areas near highly active faults, ground motions are bounded deterministically to values that are lower than ground motions for a 2475 year return period. In contrast, the design ground motion hazard in the current AASHTO Division 1-A has a probability of exceedence (PE) of 10 percent in 50 years (approx. 15% PE in 75 years or 475-year return period). With the increase in return period comes an increase in the potential for liquefaction and liquefaction-induced ground movements. These ground movements could damage bridge structures. Concerns that liquefaction hazards under the recommended provisions may prove to be too costly to accommodate in construction led to this study.

The project team believed that, along with increases in the likelihood or extent of liquefaction at a particular site, there also exists some conservatism in current design practices. If such conservatism exists, then the use of state-of-the-art design procedures could lead to designs that perform satisfactorily in larger earthquakes, and may not be much more expensive than those being currently built.

The scope of the study was limited to two sites in relatively high seismicity locations, one in the western U.S. in Washington State and one in the central U.S. in Missouri. The Washington Site is located near the Cascadia subduction zone, and the Missouri site is located near the New Madrid seismic zone. Actual site geologies and bridge configurations from the two states were used as an initial basis for the study. The site geologies were subsequently idealized by providing limited simplification, although the overall geologic character of each site was preserved.

The investigation of the two sites and their respective bridges focused on the resulting response and design differences between the recommended ground shaking level (3% PE in 75 years) and that corresponding to the current AASHTO Division I-A provisions (15% PE in 75 years). The scope of the study for each of the two sites and bridges includes:

1. Development of both 15% PE in 75 year and 3% PE in 75 year acceleration time-histories;
2. Simplified, conventional liquefaction analyses;
3. Nonlinear assessment of the site response to these accelerations including the time history of pore pressure increases;
4. Assessment of stability of abutment end slopes;
5. Estimations of lateral spreading and/or flow conditions at the sites;
6. Design of structural systems to withstand the predicted response and flow conditions;
7. Evaluation of geotechnical mitigation of liquefaction related ground displacement; and
8. Evaluation of cost impacts of the structural and geotechnical mitigation strategies.

The results for the 15% PE in 75 year and 3% PE in 75 year events were compared against one another to assess the implications of using the larger event for design. Additionally, the conduct of the study helped synthesize an overall approach for handling liquefaction-induced movements in the recommended design provisions. The study for the Washington site is described in Articles H.3

through H.8 and for the Missouri site in Article H.9, with lesser detail.

H.2 DESIGN APPROACH

The design approach used in the study and recommended for the new AASHTO LRFD provisions involves four basic elements:

1. Stability analysis;
2. Newmark sliding block analysis;
3. Assessments of the passive force that can ultimately develop ahead of a pile or foundation as liquefaction induces lateral spread; and
4. Assessment of the likely plastic mechanisms that may develop in the foundations and substructure.

The rationale behind this approach is to determine the likely magnitude of lateral soil movement and assess the structure's ability to both accommodate this movement and/or potentially limit the movement. The approach is based on use of a deep foundation system, such as piles or drilled shafts. Spread footing types of foundations typically will not be used when soil conditions lead to the possibility of liquefaction and associated lateral spreading or settlement.

The concept of considering a plastic mechanism, or hinge, in the piles under the action of spreading forces is tantamount to accepting damage in the foundation. This is a departure from seismic design for structural inertia loading alone, and the departure is felt reasonable for the rare MCE event because it is unlikely that the formation of plastic hinges in the foundation will lead to structure collapse. The reasoning behind this is that lateral spreading is essentially a displacement-controlled process. Thus the estimated soil displacements represent a limit on the structure displacement, excluding the phenomena of buckling of the piles or shafts below grade and the continued displacement that could be produced by large P-Δ effects. Buckling should be checked, and methods that include the soil residual resistance should be used. Meyersohn, et al. (1992) provides a method for checking buckling as an example. The effects of P-Δ amplification are discussed later in this Appendix.

The fact that inelastic deformations may occur below grade and that these may be difficult to detect and inspect, should be considered. However, the presence of large ground movements induced by earthquake motions is discernible. Thus, it should be possible to evaluate whether inelastic deformations could have occurred from the post-earthquake inspection information. Additionally, inclinometer tubes could be installed in selected elements of deep foundations to allow quantitative assessment of pile/shaft movement following an earthquake. Also post earthquake investigation using down hole video cameras can be used to assess damage.

A flowchart of the methodology for consideration of liquefaction induced lateral spreading is given in Figure D.4.2-1 and key components of the methodology are numbered in the flowchart and discussed in detail in the commentary to Article D.4.2.2. The figure, together with the commentary, provides a 'roadmap' to the procedure used in this study for the lateral spreading resistance design. The primary feature of the recommended methodology is the use of inelastic action in the piles to accommodate the movement of soil and foundations. If the resulting movements are unacceptable, then mitigation measures must be implemented. Mitigation measures are discussed in Article D.4.3 and are discussed in more detail in the full liquefaction report.

H.3 SITE SELECTION AND CHARACTERIZATION

Because the purpose of the study was to investigate sites that are realistic, an actual site was chosen as the prototype for a Western U.S. Site and another actual site for a mid-America site. The western site is the primary focus of this Appendix although a brief summary of the results of the Mid-America site are given in Article H.9. The Western site is located just north of Olympia, Washington in the Nisqually River valley[1]. The location is within a large river basin in the Puget Sound area of Washington State, and it is situated near the mouth of the river in the estuary zone. The basin is an area that was over ridden by

[1] This site was selected and the liquefaction evaluation was completed before the February 2001 Nisqually earthquake. Ground motions associated with the Nisqually earthquake were considerably less than those used in this study. While liquefaction occurred at some locations near the selected site no bridge damage apparently occurred likely because of the limited extent of liquefaction.

glaciers during the last ice age and therefore has over-consolidated material at depth. Additionally, the basin contains significant amounts of recently deposited, loose material over the glacially consolidated materials.

Soil conditions for the site were developed from information provided by Washington State Department of Transportation (WSDOT) for another well characterized site located in a geologically similar setting near Seattle. The actual site was moved to the Olympia area to avoid the effects of the Seattle fault. At the prototype site, the material at depths less than 150 feet are characterized by alluvial deposits. At greater depths some estuarine materials exist and below about 200 feet dense glacial materials are found. This then produces a site with the potential for deep liquefiable soils.

For the purposes of this study, the site profile was simplified such that fewer layers exist, and the profile is the same across the entire site. The simplified profile retains features and layering that produce the significant responses of the actual site. The simplified soil profile is given in Figure H.1. This figure also includes relevant properties of the soil layers that have been used for the seismic response assessments and bridge design. Shear wave velocity (V_s), undrained shearing strength (c_u), soil friction angle (φ), and residual soil strength (S_{ur}) were interpreted from the field and laboratory data provided by WSDOT. The cyclic resistance ratio (CRR) was obtained by conducting simplified liquefaction analyses using both the SPT and CPT methods to obtain CRR values. These CRR values are plotted in Figure H.2. Average CRR values were determined for liquefiable materials, and represent clean sand values for a M7.5 event.

The prototype site profile and the structure elevation are shown in Figure H.3. The modified site is a smaller river crossing than the original since the total length of the bridge was substantially shortened for the study. Only enough length was used to illustrate the issues of soil movement and design. In this case the total length of the bridge is 500 feet. The ground surface is shown in Figure H.3 as the 0-foot elevation. As can be seen in the figure, approach fills are present at both ends of the bridge, and in this case, they are relatively tall at 30-feet each.

An approach fill comprised of a relatively clean sandy gravel was assumed at each abutment. The sandy gravel was assigned a friction angle of 37 degrees.

H.4 BRIDGE TYPE

The prototype bridge from which the study data were drawn is a river crossing with several superstructure and foundation types along the structure. Again for the study, the actual structure was simplified. The 500-foot long structure comprises of a 6-foot deep concrete box girder that is continuous between the two abutments. The intermediate piers are two-column bents supported on pile caps and 24-inch steel piles filled with reinforced concrete. The roadway is 40-feet wide. The two 4-foot diameter columns for each pier are approximately 23 feet apart, and due to the relatively large size of the pile caps, a single combined pile cap was used for both columns at each pier. Figure H.4 shows the general arrangement of an intermediate pier.

The centermost pier in this example is located at the deepest point of the river channel, as shown in Figure H.3. While this is somewhat unusual, in that a longer span might often be used to avoid such an arrangement, the river pier was used here for simplicity. The columns of this pier are also relatively slender, and they were deliberately left so to allow any negative seismic effects of the slenderness, for instance P- , to be assessed. In a final design, the size of these columns might likely be increased. In fact, non-seismic load combinations/conditions may require the columns to be enlarged.

WASHINGTON SITE
Non-Liquefied Soil Profile

<table>
<tr><th>Elevation feet</th><th>Soil Type</th><th>Shear Velocity V_s (fps)</th><th>Cohesion c_u (psf)</th><th>Friction Angle ϕ (degrees)</th><th>Cyclic Resist. Ratio CRR</th><th>Res. Strength S_{ur}</th></tr>
<tr><td>31.0</td><td>1 Sand (Fill)</td><td rowspan="9">550</td><td></td><td>37</td><td></td><td></td></tr>
<tr><td>0.0</td><td>2 Soft Clay</td><td>1000</td><td></td><td></td><td></td></tr>
<tr><td>-10.0</td><td>3 Sand *</td><td></td><td>38</td><td>0.15</td><td rowspan="7">300</td></tr>
<tr><td>-15.0</td><td>4 Sand</td><td></td><td>40</td><td>0.2</td></tr>
<tr><td>-25.0</td><td>5 Sand</td><td></td><td>42</td><td>0.3</td></tr>
<tr><td>-30.0</td><td>6 Sand</td><td></td><td>32</td><td>0.15</td></tr>
<tr><td>-35.0</td><td>7 Sand</td><td></td><td>40</td><td>0.2</td></tr>
<tr><td>-40.0</td><td>8 Soft Clay</td><td>1000</td><td></td><td></td></tr>
<tr><td>-45.0</td><td>9 Sand *</td><td></td><td>38</td><td>0.15</td></tr>
<tr><td>-50.0</td><td>10 Sand</td><td>650</td><td></td><td>32</td><td>0.15</td><td>500</td></tr>
<tr><td>-100.0</td><td>11 Stiff Clay w/o Free Water</td><td>700</td><td>2000</td><td></td><td></td><td></td></tr>
<tr><td>-150.0</td><td>12 Stiff Clay w/o Free Water</td><td>750</td><td>2500</td><td></td><td></td><td></td></tr>
<tr><td>-200.0</td><td>Till</td><td>1500</td><td></td><td></td><td></td><td></td></tr>
</table>

* Liquefiable Sand

Figure H-1 Simplified Soil Profile for the Western U.S. Site

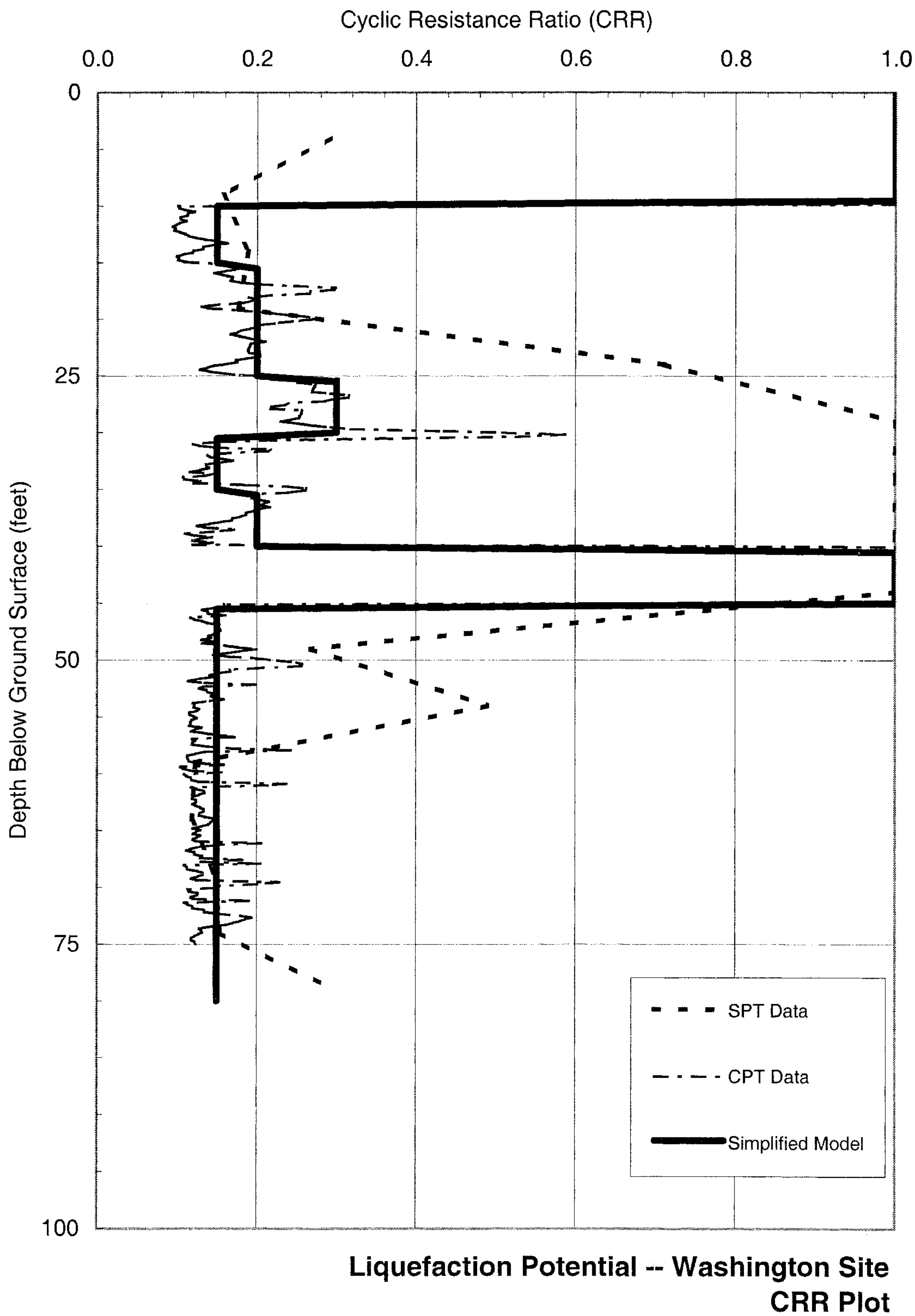

Figure H.2 WSDOT Location H-13 CRR Plot

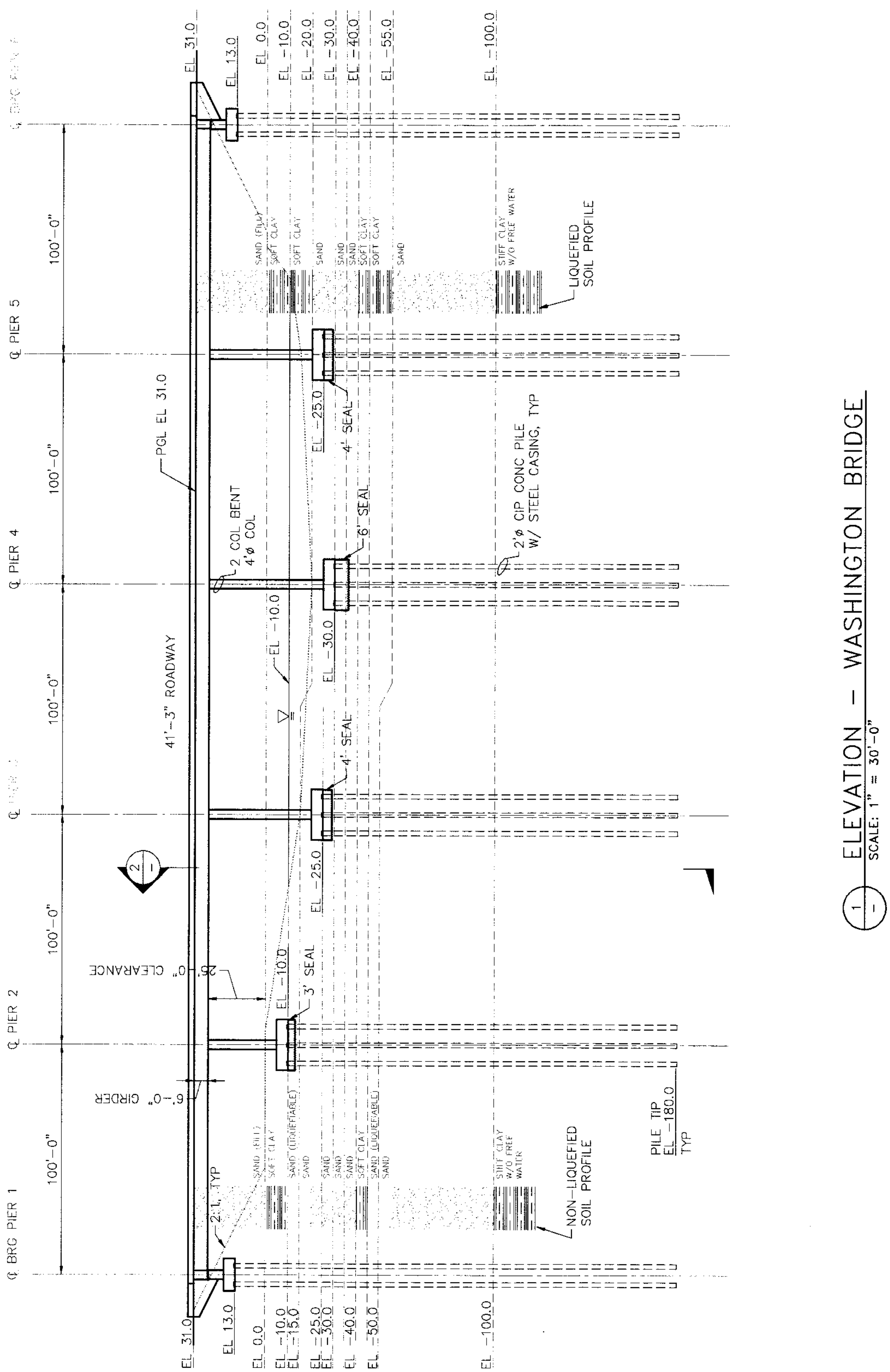

Figure H.3 Site Profile and Structure Elevation

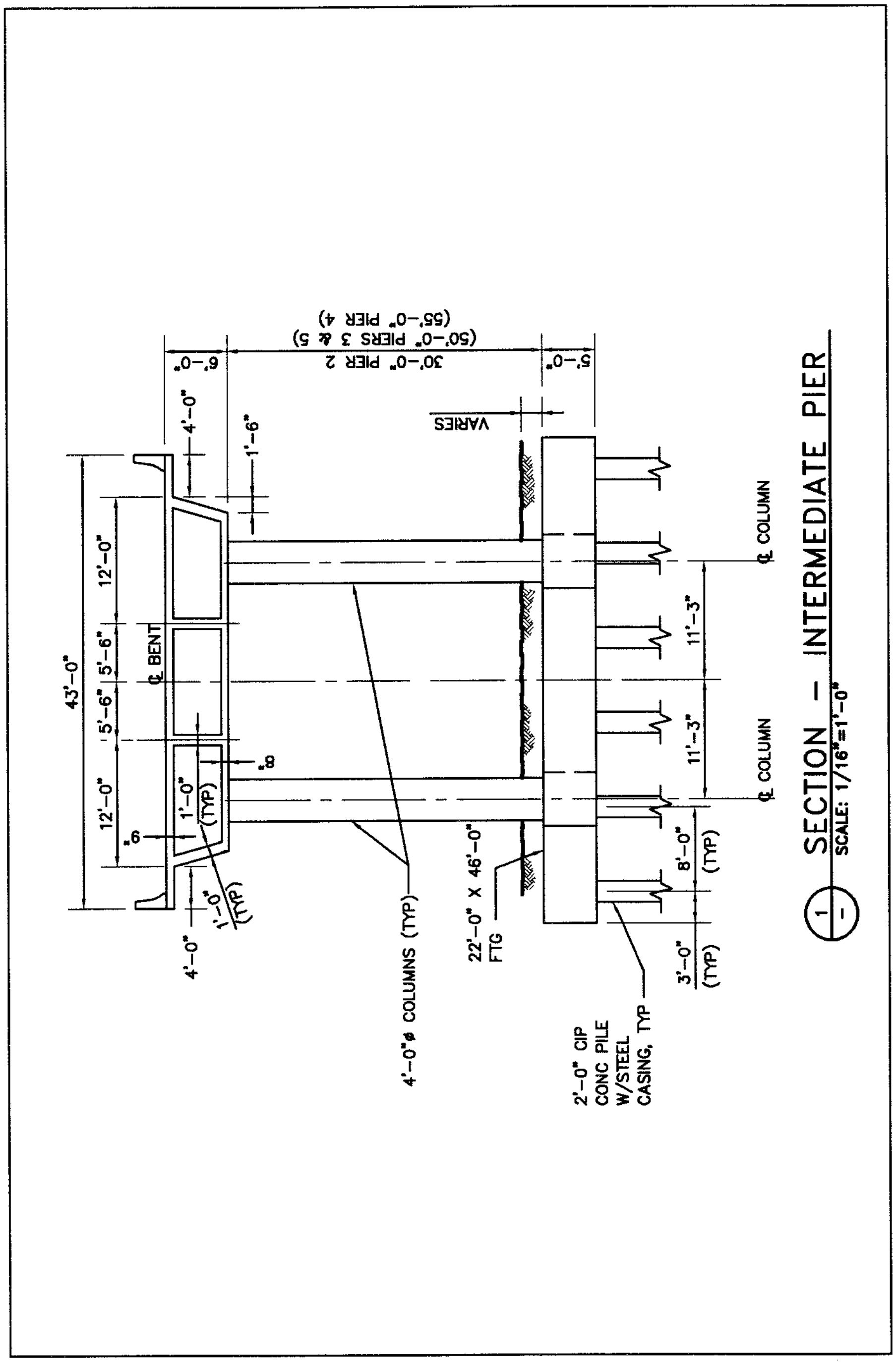

Figure H-4 Elevation of an Intermediate Pier

The abutments are of the overhanging stub abutment type. Figure H.5 shows the transverse and longitudinal elevations of the abutments used for the bridge. For this type of abutment, the backfill is placed directly against the end diaphragm of the superstructure. This has the seismic advantage of providing significant longitudinal resistance for all displacement levels, since the passive resistance of the backfill is mobilized as the superstructure moves. This type of abutment also eliminates the need for expansion joints at the ends of the structure, and for this reason, is limited to the shorter total length structures.

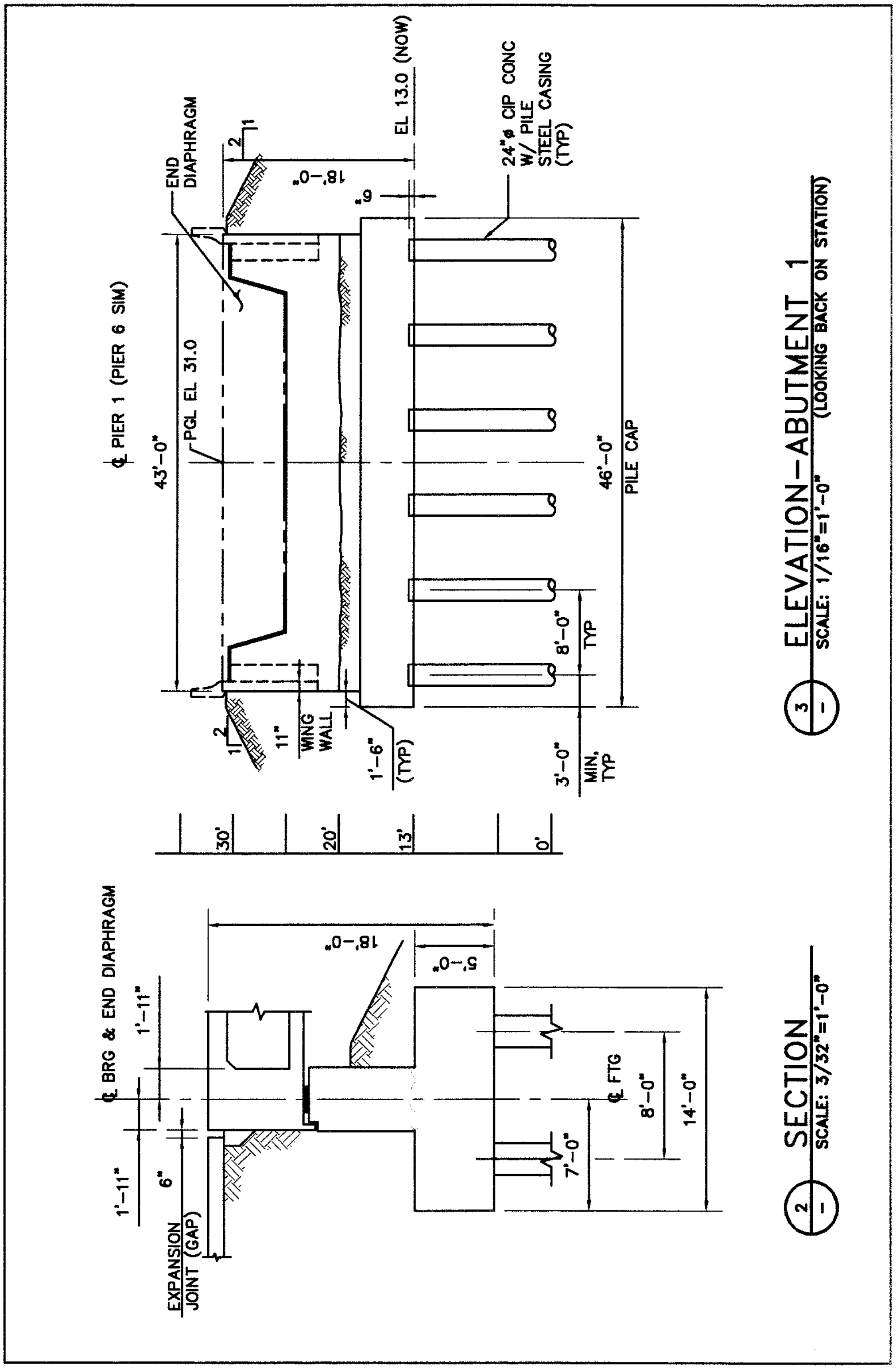

Figure H.5 **Elevations of the Abutment**

H.5 DESIGN RESPONSE SPECTRA AND TIME HISTORIES

The design response spectra for current AASHTO Specifications and recommended LRFD provisions were constructed using the procedures and site factors described in the respective specifications. For current AASHTO Specifications, the hazard level of 10% probability of exceedance in 50 years was used. For the recommended LRFD Specifications, both the rare earthquake (Maximum Considered Earthquake or MCE) having a probability of exceedance of 3% in 75 years with deterministic bounds near highly active faults and the frequent earthquake (also termed the expected earthquake) having a probability of exceedance of 50% in 75 years were used as design earthquakes

Design response spectra based on current AASHTO Specifications were constructed using a (rock) peak ground acceleration (PGA) of 0.24g for the Olympia site. This peak ground acceleration value was determined from the AASHTO map contained in the current AASHTO Specifications. Design spectra for the MCE of the recommended LRFD Specifications were constructed using rock (Site Class B) spectral accelerations at 0.2-second period and 1.0-second period. These two spectral values were obtained from maps published by the U.S. Geological Survey (USGS). The PGA for the MCE was defined as 0.4 times the spectral acceleration at 0.2 seconds as required by the recommended LRFD provisions. Design spectral accelerations for the expected earthquake were obtained from the hazard curves of probabilistic ground motions on the CD-ROM published by the USGS.

Rock spectra based on AASHTO and the recommended LRFD provisions were adjusted for local site soil conditions. According to the AASHTO specifications the site is a Soil Profile III; the recommended LRFD provisions define the site as Class E. Figure H.6 presents the design response spectra for current AASHTO Specifications, on Soil profile Type III, and for the MCE and the frequent earthquake of the recommended LRFD Specifications, on Site Class E. These site classifications represent the assessed soil profile below the ground surface where response spectra are defined for structural vibration design and peak ground accelerations are used for simplified liquefaction potential analyses. Note in Figure H.6 that the short-period branch of the AASHTO spectra are assumed to drop from the acceleration plateau at a period of 0.096 second to the peak ground acceleration at 0.02-second period, the same as for the MCE spectra. Also note that, because the long-period branch of the AASHTO spectra declines more slowly with period than those of the MCE (as $1/T^{2/3}$ in AASHTO compared to 1/T in the recommended LRFD Specifications), the AASHTO and MCE spectra come closer together as the period increases.

Acceleration time histories consistent with current AASHTO Specifications and with MCE ground motions of the recommended LRFD Specifications were developed as firm soil outcropping motions for input to the one dimensional, non-linear site response analyses to assess the liquefaction hazard of the site. These time histories were developed in accordance with the requirements and guidelines of the recommended LRFD provisions. Deaggregation of the probabilistic results for the Olympia site indicates that significant contributions to the ground motion hazard come from three magnitude-distance ranges: (1) magnitude 8 to 9 earthquakes occurring at a distance of 70 to 80 km distance; (2) magnitude 5 to 7 events occurring at a distance of 40 to 70 km distance; and (3) magnitude 5 to 6.5 earthquakes occurring at distances less than 20 km. These three magnitude-distance ranges are associated respectively, with (1) large-magnitude subduction zone interface earthquakes, (2) moderate magnitude earthquakes occurring within the subducting slab of the Juan de Fuca plate at depth beneath western Washington and in the shallow crust of the North American plate at relatively large distances from the site, and (3) moderate magnitude earthquakes occurring in the shallow crust of the North American plate in the near vicinity of the site. Time histories were developed for each of these earthquake sources. The selected source for (1) was the 1985 Chile earthquake, for (2) it was representative of the events occurring within the subducting slab, of the type that occurred near Olympia in 1949 and 2001 Nisqually earthquake, and for (3) it was 1986 North Palm Springs earthquake, a moderate magnitude local shallow crustal earthquake.

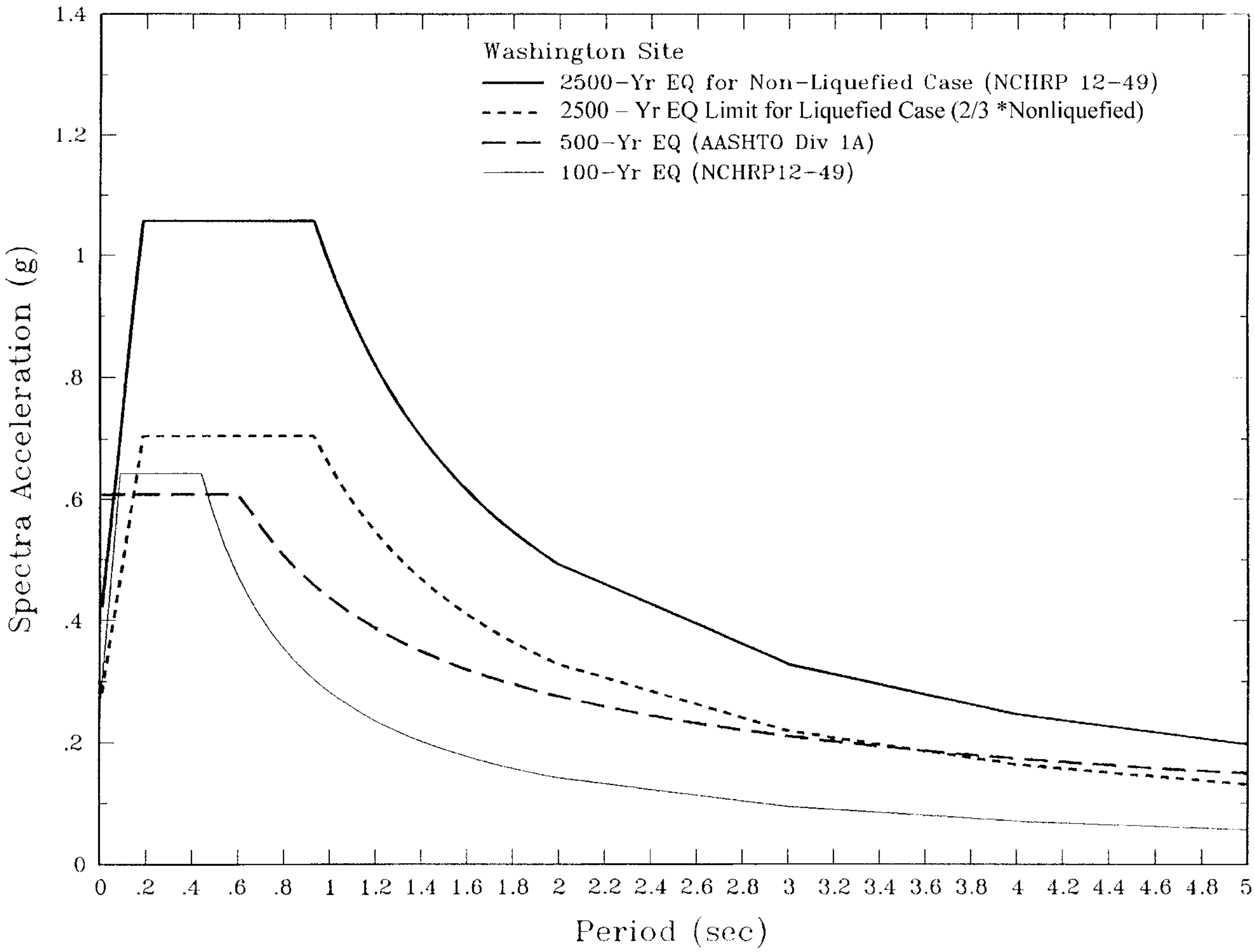

Figure H.6 Design Response Spectra Based on Current AASHTO Specifications, Site Class III, and the MCE and the Frequent Earthquake of Proposed LRFD Specifications, Site Class E, Washington Site

H.6 LIQUEFACTION STUDIES

The liquefaction study for the Washington bridge site involved two phases. In the first, a series of liquefaction analyses were conducted using the SPT and CPT simplified methods. Results of these analyses were used to determine the depths at which liquefaction could occur during the 15% PE in 75 year and 3% PE in 75 year earthquakes. These results were also used as a basis for determining the residual strength of the soil. Concurrent with these analyses, a series of one-dimensional nonlinear, effective stress analyses was conducted to define more explicitly the mechanisms for pore water pressure increase within the soil profile and the changes in ground accelerations and deformations resulting from the development of liquefaction.

H.6.1 Simplified Liquefaction Analyses

The first step of the procedure outlined in the commentary to Article D.4.2.2 is to determine whether liquefaction is predicted to occur.

Simplified liquefaction analyses were conducted using the procedures given in Youd and Idriss (1997). Two levels of peak ground acceleration (PGA) were used, one representing the acceleration from the current AASHTO LRFD with its 10% PE in 50 year event and the other representing the recommended 3% PE in 75 year event. The PGA for the 10% in 50 year event was not adjusted for site effects: this is consistent with the approach recommended in the current AASHTO Standard Specifications[2]. Ground motions for the 3% PE in 75 year event were adjusted to Site Class E, as recommended in Article 3.4. The resulting PGA values for each case are summarized below.

Input Parameter	10% PE in 50 Years	3% in 75 Years
Peak ground acceleration	0.24g	0.42g
Mean Magnitude	6.5	6.5

The magnitude of the design earthquake was required for the SPT and CPT simplified analyses. Results of deaggregation studies from the USGS database suggest that the mean magnitude for PGA for the 10% PE in 50 year and 3% in 75 year events is 6.5. This mean magnitude reflects contributions from the different seismic sources discussed above. However, common practice within the State of Washington has been to use a magnitude 7.5 event, as being representative of the likely size of a subduction zone event occurring directly below the Puget Sound area. In view of this common practice, a range of magnitudes (6.5, 7.0 and 7.5) was used during the liquefaction analyses.

For these analyses, ground water was assumed to occur 10 feet below the ground surface for the non-fill case. Evaluations were also performed using a simplified model to evaluate the effects of the fill. For the fill model, the soil profile with the associated soil properties was the same as the free-field case. However, an additional 30 feet of embankment was added to the soil profile. This change results in a lower imposed shearing stress (i.e., demand) because of the lower soil flexibility factor (R_d). No adjustments were made to the normalized CRR values for the greater overburden. As discussed in Youd and Idriss (1997), the recommended approach for a site where fill is added is to use the pre-fill CRR value, under the assumption that the overburden effects from the fill will not have an appreciable effect on the density of the material.

Factors of safety (FOS) results from the liquefaction evaluations at the three magnitudes (6.5, 7.0 and 7.5) are shown in Figure H.7a and H.7b for the 10% PE in 50 year and 3% PE in 75 year seismic events, respectively, for the case of no approach fill. These results indicate that liquefaction could occur at two depths within the soil profile for the 10% PE in 50 year ground motion, depending somewhat on the assumed earthquake magnitude. For the 3% PE in 75 year event liquefaction is predicted to depths of 75 feet, regardless of the assumption on the earthquake magnitude[3].

Results of the liquefaction analyses with the approach fill are compared in NCHRP Liquefaction Study Report (NCHRP 2000). The fill case results in somewhat lower liquefaction potential (i.e., higher FOS) due to the lower imposed shearing stress.

H.6.2 DESRA-MUSC Ground Response Studies

A more detailed and refined approach to assess if liquefaction occurs and the resulting ground motion is to use a nonlinear dynamic effective stress approach. For this assessment, one-dimensional nonlinear effective stress site response analyses were conducted using the program DESRA-MUSC (Martin and Ping, 2000).

[2] Common practice is to adjust the PGA for the site soil factors given in Table 2 of Division 1-A. While this adjustment may be intuitively correct, these site factors are not explicitly applied to the PGA. If the site coefficient were applied at the Washington site, the PGA would be increased by a factor of 1.5, making it only slightly less than the PGA for the 2,475-year event.

[3] The maximum depth of liquefaction was cut-off at 75 feet, consistent with WSDOT's normal practice. There is some controversy whether a maximum depth of liquefaction exists. Some have suggested that liquefaction does not occur beyond 55 feet. Unfortunately, quantitative evidence supporting liquefaction beyond 55 feet on level ground is difficult to find; however, cases of deep liquefaction were recorded in the 1964 Alaskan earthquake. For expediency liquefaction in the simplified analysis was limited to 75 feet.

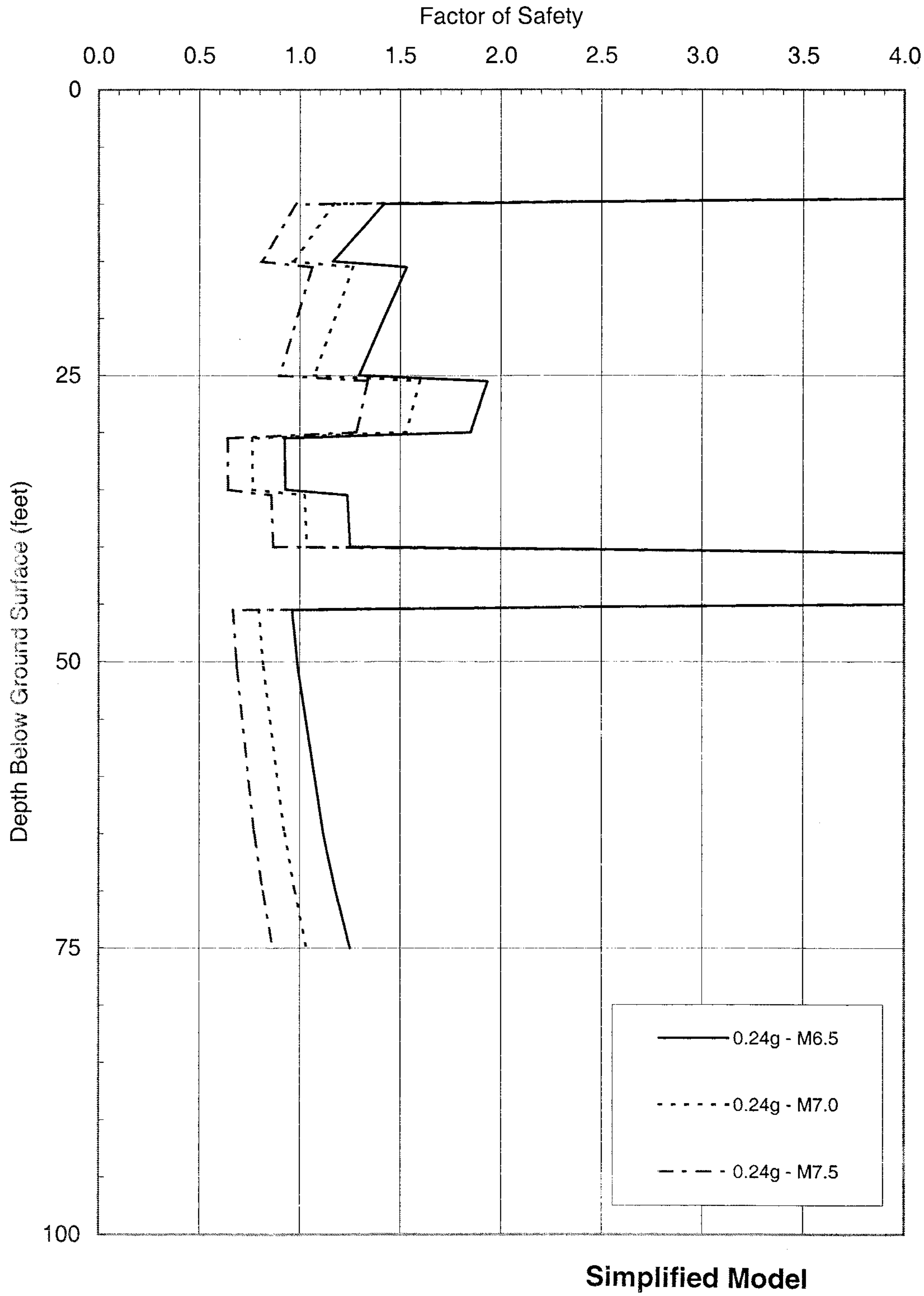

Figure H.7a **Liquefaction Potential – 475-Year Return Period**

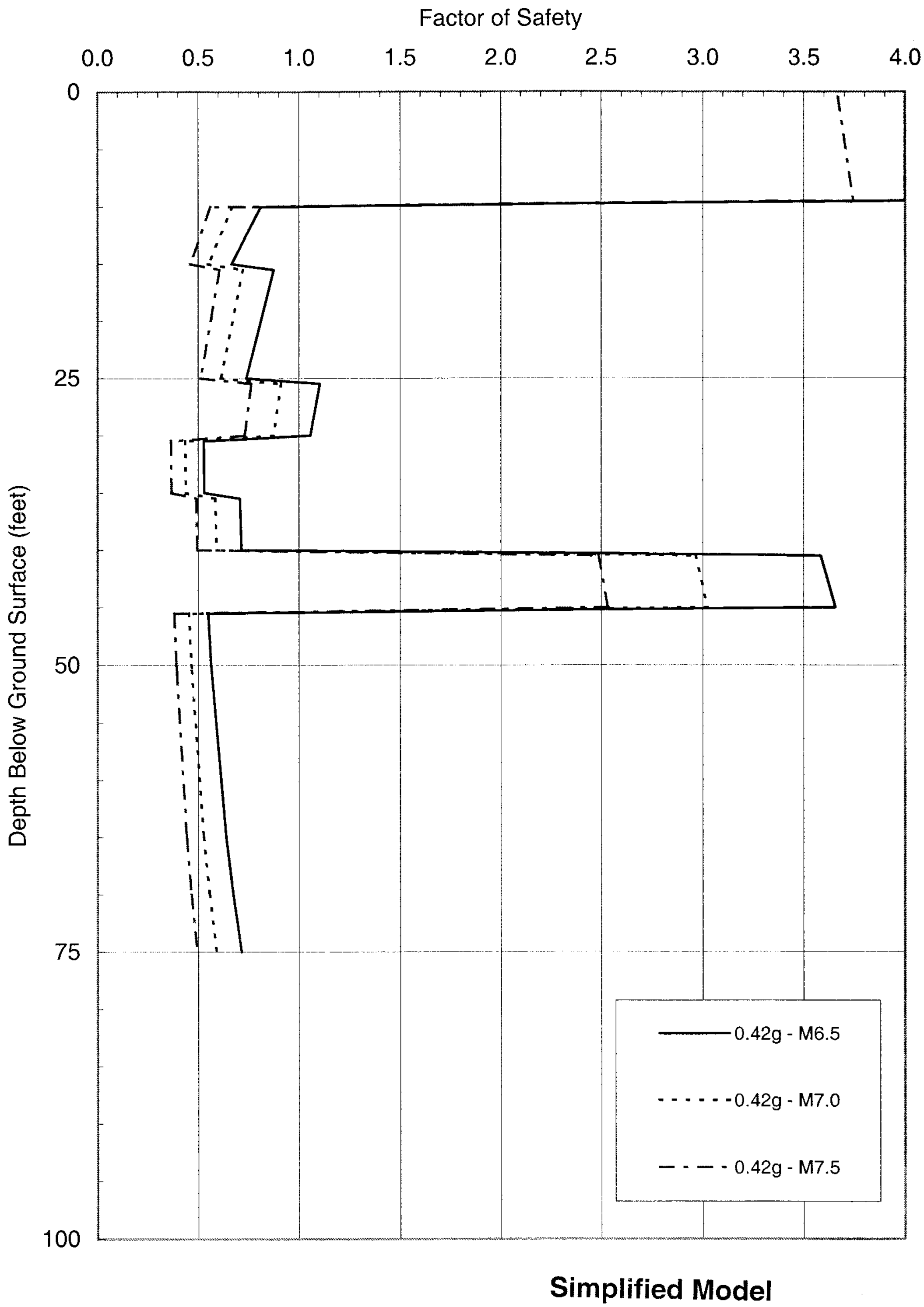

Figure H.7b Liquefaction Potential – 2,475-Year Return Period

The idealized site profile and related soil properties adopted for the response analyses are shown in Figure H.1. Response analyses were performed for the three ground motions, assuming a transmitting boundary input at a depth of 200 feet, corresponding to the till interface. Analyses were conducted for both the 10% PE in 50 year and 3% PE in 75 year events and for site profiles with and without embankment fill. The DESRA-MUSC parameters utilized for analyses for the various soil strata (G/G_{max} curves, backbone curves and liquefaction strength curves) are documented in the case study report together with the results of response analyses for all cases defined above. A representative set of results for the time history matching the site spectra, but based on the 1985 Chile Earthquake, which has the highest energy levels of the three events used for analyses (representative of a M 8 event) are described below.

H.6.2.1 Without Embankment Fill

The site response for the 10% in 50 year earthquake is summarized in four figures:

- Figure H.8 - input and output acceleration time histories and response spectra
- Figure H.9 - maximum shear strains induced as a function of depth
- Figure H.10 - time histories of pore water pressure generation at various depths
- Figure H.11 - shear stress-shear strain hysteretic loops at various depths

A similar set of figures summarize data for the 3% PE in 75 year earthquake. The following are key observations from the data plots:

- The pore water pressure time history response and output accelerations are very similar for the 10% PE in 50 year and 3% PE in 75 year cases. The underlying reason for this is the fact that the higher input accelerations for the 3% PE in 75 year case are more strongly attenuated when transmitted through the clayey silts between 100 to 200 feet, such that input accelerations at the 100-foot level for both cases, are of the order of 0.25g.

- All liquefiable soils between 10 and 100 feet eventually liquefied for both cases. However liquefaction was first triggered in the 45- to 50-foot layer, which became the focal point for shear distortion and associated ground lurch (see Figure H.9 and H.11). Maximum shear strains of about 6 and 10% for the 10% PE in 50 year and 3% PE in 75 year events, respectively, over the 5-foot depth of this layer, would suggest maximum ground lurches of about 0.3 and 0.5 feet respectively. Liquefaction also occurred at about the same time for the layer between 10 and 20 feet. Maximum shear strains in this and other layers were relatively small, but still sufficient to eventually generate liquefaction. The strong focal point for shear strains for the 45- to 50-foot layer suggests that this layer would also be the primary seat of lateral spread distortion.

- Liquefaction at the 45- to 50-foot depth, which was triggered at about a time of 17 seconds, effectively generated a base isolation layer, subsequently suppressing the transmission of accelerations above that depth, and generating a much “softer” soil profile. This is graphically illustrated in Figure H.8 which shows suppression of input accelerations and longer period response after about 17 seconds. Such behavior is representative of observations at sites, that liquefied during the Niigata and Kobe earthquakes.

Similar trends to those described above were seen for the other two time histories based on the Olympia and Desert Hot Springs earthquakes. However, for the Desert Hot Spring event, more representative of a M6.5 event, liquefaction did not occur at depths greater than 55 feet and only barely occurred at depth between 20 and 30 feet, for the 475-year event.

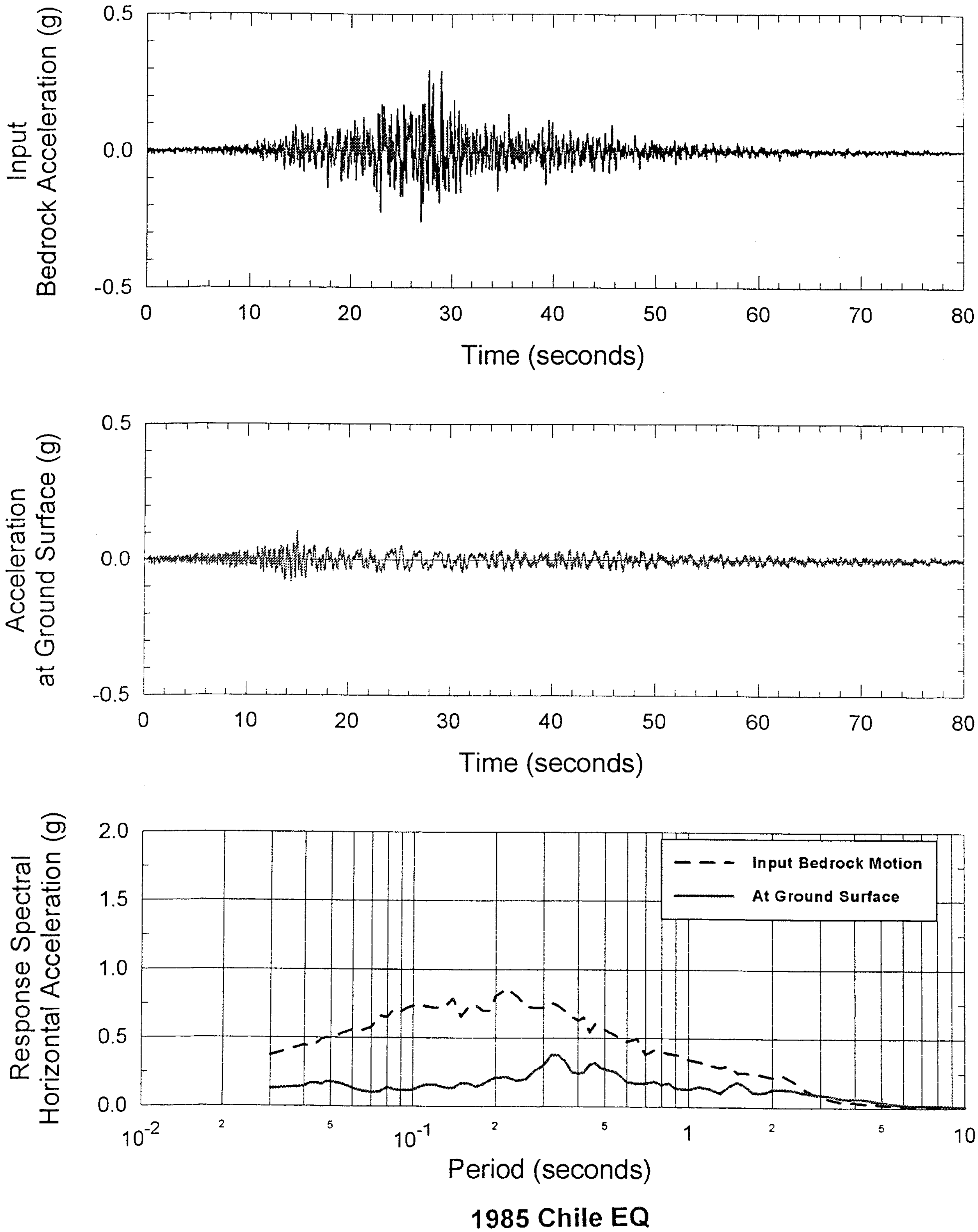

Figure H.8 Input and Output Acceleration Histories and Response Spectra, 475-Year Earthquake Without Fill

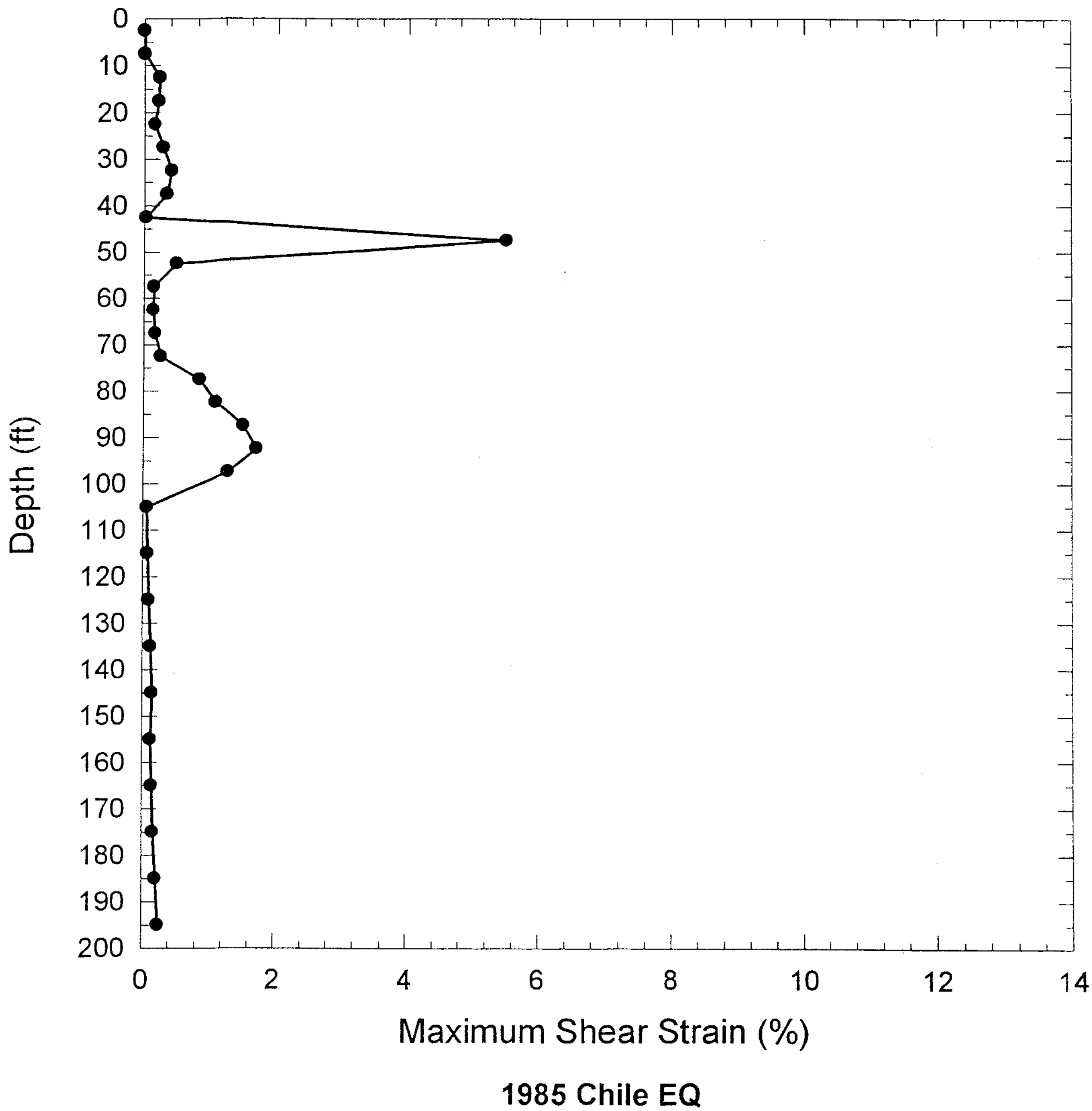

Figure H.9 Maximum Shear Strains Induced as a Function of Depth, 475-Year Earthquake Without Fill

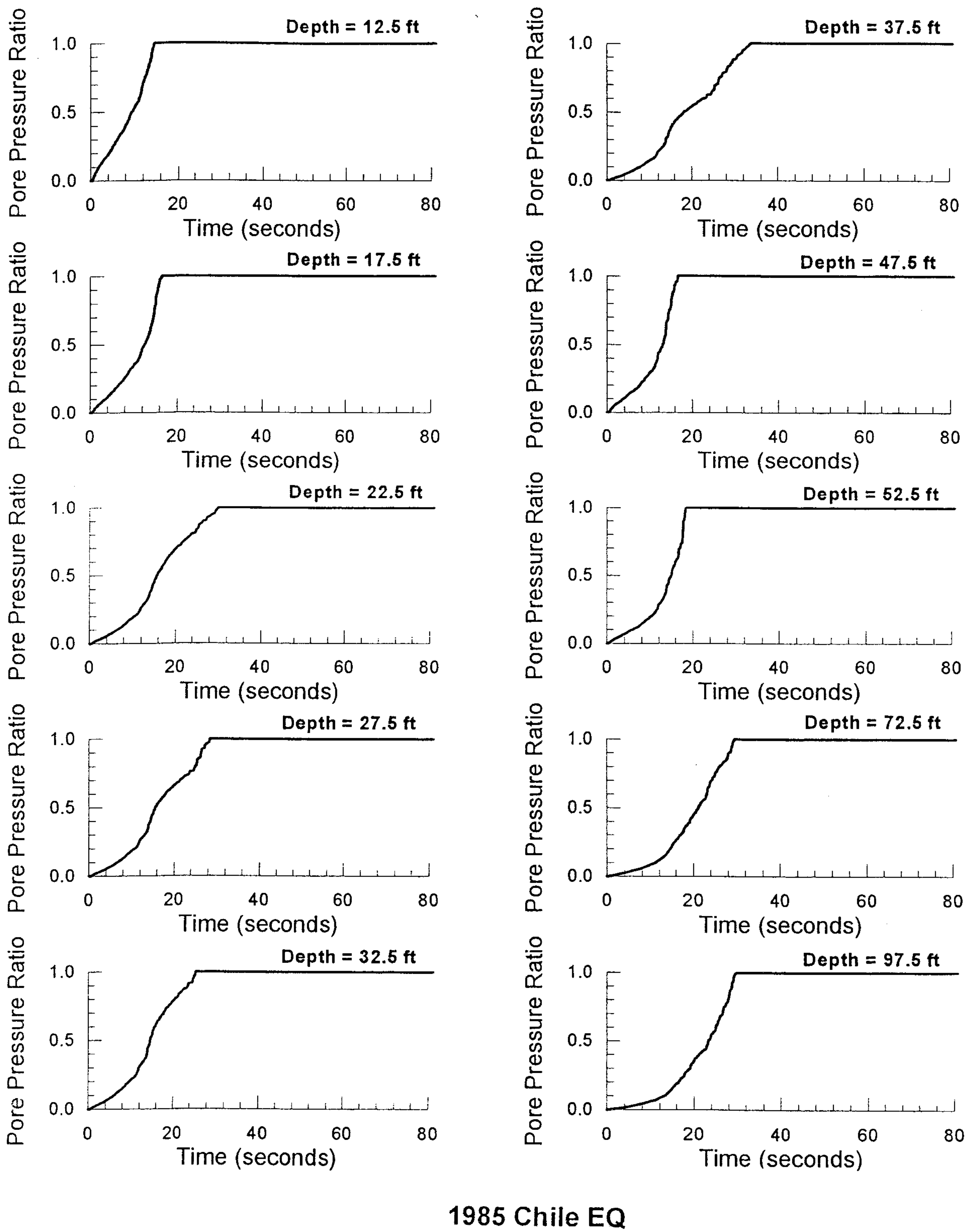

Figure H.10 Time Histories of Pore Pressure Generation at Various Depths, 475-Year Earthquake Without Fill

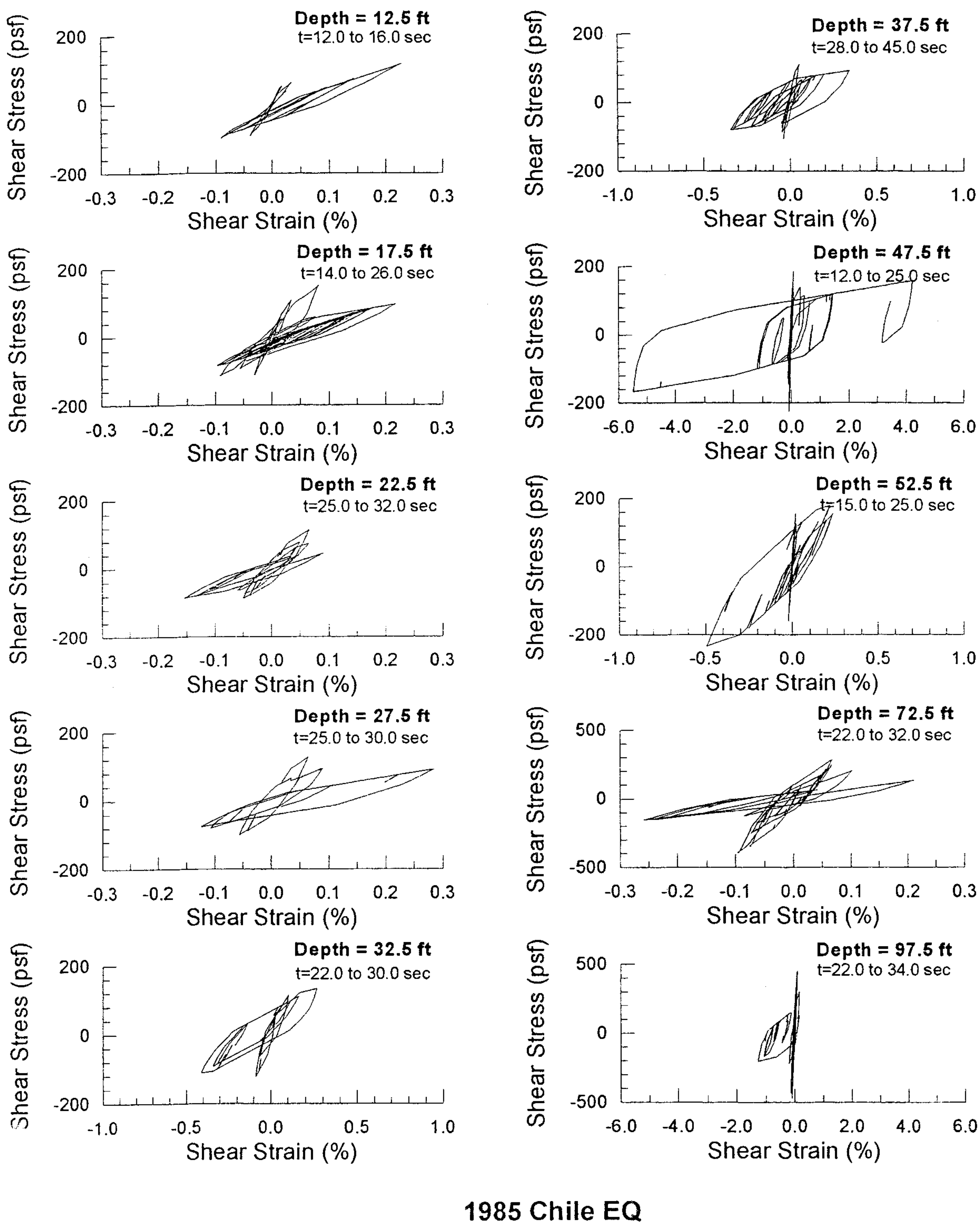

Figure H.11 Shear Stress – Shear Strain Hysteretic Loops at Various Depths, 475-Year Earthquake Without Fill

The above results are generally consistent with the factor of safety calculations using the simplified method. However, one notable difference is the observation that the sand layer between 25 and 30 feet (CRR = 0.3) tends to build up pore water pressure and liquefy in a similar manner to the layers above (CRR = 0.2) and below (CRR = 0.15) due to pore water pressure redistribution effects in DESRA-MUSC, whereas the simplified method which assumes no drainage during earthquake shaking, indicates factors of safety greater than one for 475-year events. The effects of redistribution, also tend to suppress the rate of pore water pressure build up in the layer between 30 and 35 feet.

H.6.2.2 With Embankment Fill

The site response for the 475- and 2,475-year earthquakes is summarized in a similar manner to the no fill case above. As in the simplified method, the effect of the fill is to suppress the rate of pore water pressure build up in the DESRA-MUSC analyses (or increase factor of safety in the case of the simplified method). However, the overall response is similar for both the 10% PE in 50 year and 3% PE in 75 year cases, as for the no fill case.

Liquefaction was first triggered in the 45 to 50-foot layer, which became the focal point for shear distortion as in the no fill case. Liquefaction also occurred at about the same time for layers between 10 and 20 feet. However, liquefaction was suppressed in layers between 20 and 40 feet. The strong focal point for shear strains for the 45- to 50-foot layers, again suggests that this layer would be the primary seat of lateral spread distortion. Similar trends to those described above were also seen for the time histories based on the Olympia and Desert Hot Spring earthquakes, although as for the no fill case, liquefaction did not occur at depths greater than 55 feet for the 475-year Desert Hot Springs event.

The above results are again generally consistent with the factor of safety calculations using the simplified method, but with the notable differences that for the 475-year Olympia and Chile events, liquefaction occurred at depths between 70 and 100 feet, whereas factors of safety would have been greater than one based on the simplified method. This reflects the "bottom up" wave propagation used in DESRA-MUSC, versus the "top down" inertial loading from the simplified method.

H.6.3 Lateral Ground Displacement Assessment

From the results of the simplified liquefaction studies, two liquefiable zones were identified for stability and displacement evaluations. One extends from a depth of 10 feet to 20 feet below the ground surface. The other extends from 45 to 55 feet below the ground surface. The residual strength of these two liquefied zones was selected as 300 psf based on the SPT blow counts in each layer. Soils between 20 and 40 feet below the ground surface and between 55 and 100 feet below the ground surface were assumed to have partial build-up in pore water pressure, resulting in some reduction in the friction angle of the non-liquefied sand layers, as shown in the DESRA-MUSC analyses. For these conditions, the response of the end slope for the approach fill on each side of the channel was estimated by conducting pseudo-static stability evaluations followed by simplified deformation analyses using chart- based Newmark analyses. These correspond to Steps 2 and 3 of the design procedure of Article D. 4.2.2.

H.6.3.1 Initial Stability Analyses

Once liquefaction has been determined to occur, a stability analysis is performed to assess the potential for soil movement as indicated in Step 2 of the design procedure.

The computer program PCSTABL was used during these analyses. Most analyses were conducted using a simplified Janbu failure method of analysis with a wedge failure surface. This geometry was believed to be most representative of what would likely develop during a seismic event. Checks were also performed for a circular failure surface and using the modified Bishop and Spencer methods of analysis. Both pre-liquefaction and post-liquefaction strengths were used during these analyses.

Results of the pre-liquefaction studies indicate that the static FOS for the end slopes on each side of the channel were 1.5 or more, confirming acceptable static conditions. Yield accelerations (accelerations that produce FOS's of 1 on postulated failure surfaces in the pre-liquefaction state) were typically greater than 0.15, suggesting that some deformation would occur within the end slopes, even without liquefaction.

The FOS values dropped significantly when residual strengths were assigned to the two liquefied layers, as summarized in the following table. For these analyses the geometry of the failure surfaces was constrained to force failure through the upper or lower liquefied zone. Results given in the following table are for post-liquefaction conditions; i.e., no seismic coefficient for the right-hand approach fill.

Case	Abutment	Factor of Safety	Comment
Upper Wedge	Right	0.71	Modified Janbu
Lower Wedge	Right	0.79	Modified Janbu
Upper Circle	Right	0.81	Modified Bishop
Lower Circle	Right	0.86	Modified Bishop

Results of the stability analyses for the right-hand abutment indicate that for liquefied conditions and no inertial force in the fill (i.e., after the earthquake), factors of safety range from 0.7 to 0.9 for different assumptions of failure surface location and method of analysis. FOS values less than 1.0 indicate that lateral flow failure of the material is expected during any event that causes liquefaction in the two layers, whether it is associated with the 10% PE in 50 year or 3% PE in 75 year event. The potential for instability is similar for failure surfaces through the upper and lower layers of liquefied soil, suggesting that any mitigation procedure would have to consider displacements through each layer. In other words, it would not be sufficient to improve only the upper 20 feet of soil where the FOS was lower, as a liquefaction-related failure could also occur at deeper depths.

Given the predicted occurrence of a liquefaction-induced flow failure, it would be desirable to quantify the amount of displacement expected during this flow, which corresponds to Step 3 of the design procedure. Unfortunately, this is quite difficult when flow failures are predicted to occur. The simplified chart methods or the Newmark time history analysis, cannot be used to compute displacements for flow failures. However, flow displacements could be expected to be large, and such large displacements would indicate mitigation might be needed. More detailed analyses considering both structural pinning effects and ground modifications for mitigation of displacements are discussed in the following section of this Appendix.

H.6.3.2 Lateral Spread Implications from DESRA-MUSC Analyses

A key conclusion from the DESRA-MUSC analyses was the strong likelihood that lateral spread deformations would be controlled by a failure zone in the 45- to 50-foot layer. Displacement time histories for a rigid block sliding on this layer (assuming a Newmark sliding block analogy) were generated for a range of yield accelerations, using input acceleration time histories generated at the base of the 50- to 55-foot layer. The analyses were performed using the DISPMNT computer program (Houston et. al., 1987). "Upslope" deformations were suppressed assuming a strong one directional driving force from the embankment. At time zero, drained strengths for the liquefied layer were assumed. Strengths were degraded as a function of pore water pressure increase and reduced to the assumed residual strength of 300 psf when liquefaction was triggered. As would be expected, most of the computed displacements occurred subsequent to triggering.

Results showing displacement time history plots for the 3% PE in 75 year event based on the Chile earthquake as a function of yield acceleration, are shown in Figure H.12. Total accumulated displacements as a function of yield acceleration are shown in Figure H.13 for the three earthquake records. These plots became a basis for discussion on remediation analyses, as described in Article H.6.3.4. Similar analyses for potential failure surfaces in the depth zone of 10 to 20 feet, gave a maximum displacement of only 0.06 feet.

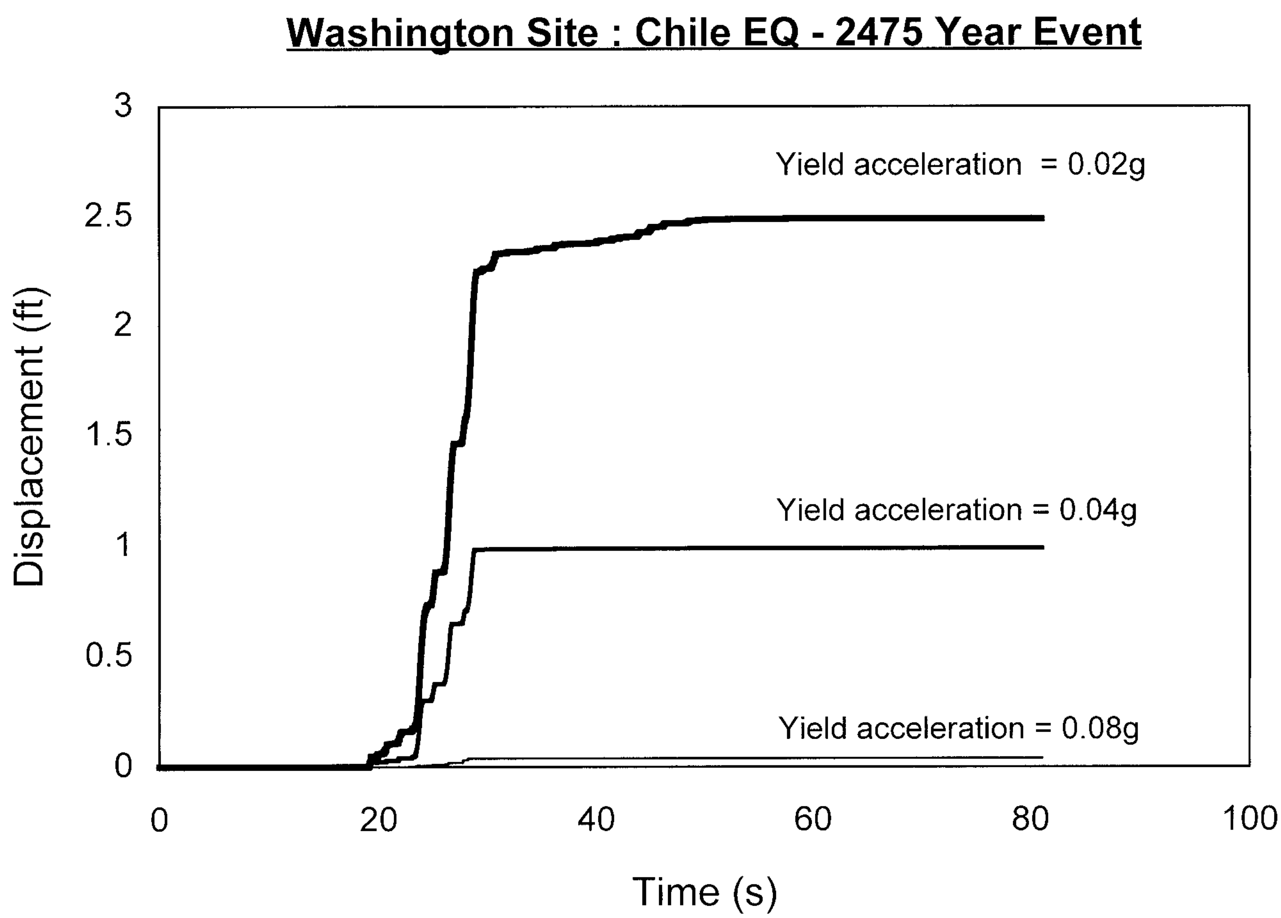

Figure H.12 Displacement vs. Time for 2475-Year Earthquake

H.6.3.3 Stability Analyses with Mitigation Measures

Since it has been determined that significant soil movements will occur, Step 7 of the design procedure requires an evaluation of measures that will reduce the amount of movement.

Two procedures were evaluated for mitigating the potential for lateral flow or spreading, structural pinning and ground improvement. For these analyses the additional resistance provided by the improved ground or by the structural pinning of the soil was incorporated into the stability analyses described above. If the FOS for the revised analysis was greater than 1.0, the yield acceleration for the mitigated condition was determined, which then allowed displacements to be estimated. If the FOS was still less than 1, then flow would still occur and additional mitigation measures would be required.

For the structural pinning evaluation, shear forces were calculated to be 90 kips per pile for sliding on either the upper or lower failure surfaces. Procedures for determining the amount of pinning force are given in Article H.7.2. The abutment has 12 piles which extend through the sliding zone, resulting in 1,080 kips of additional shear reaction to sliding. Pier 5 of the bridge has 16 piles that produce 1,440 kips of pinning force. The abutment and the columns for Pier 5 are expected to develop reaction forces from passive pressure and column plastic shear. These forces were calculated to be 400 kips and 420 kips, respectively. This reaction occurs over the 48-feet abutment and pile cap widths, resulting in a total resistance of 31 and 70 kips per foot of width (or 1480 kips and 3340 kips, total) for displacement along the upper and lower liquefied zones, respectively.

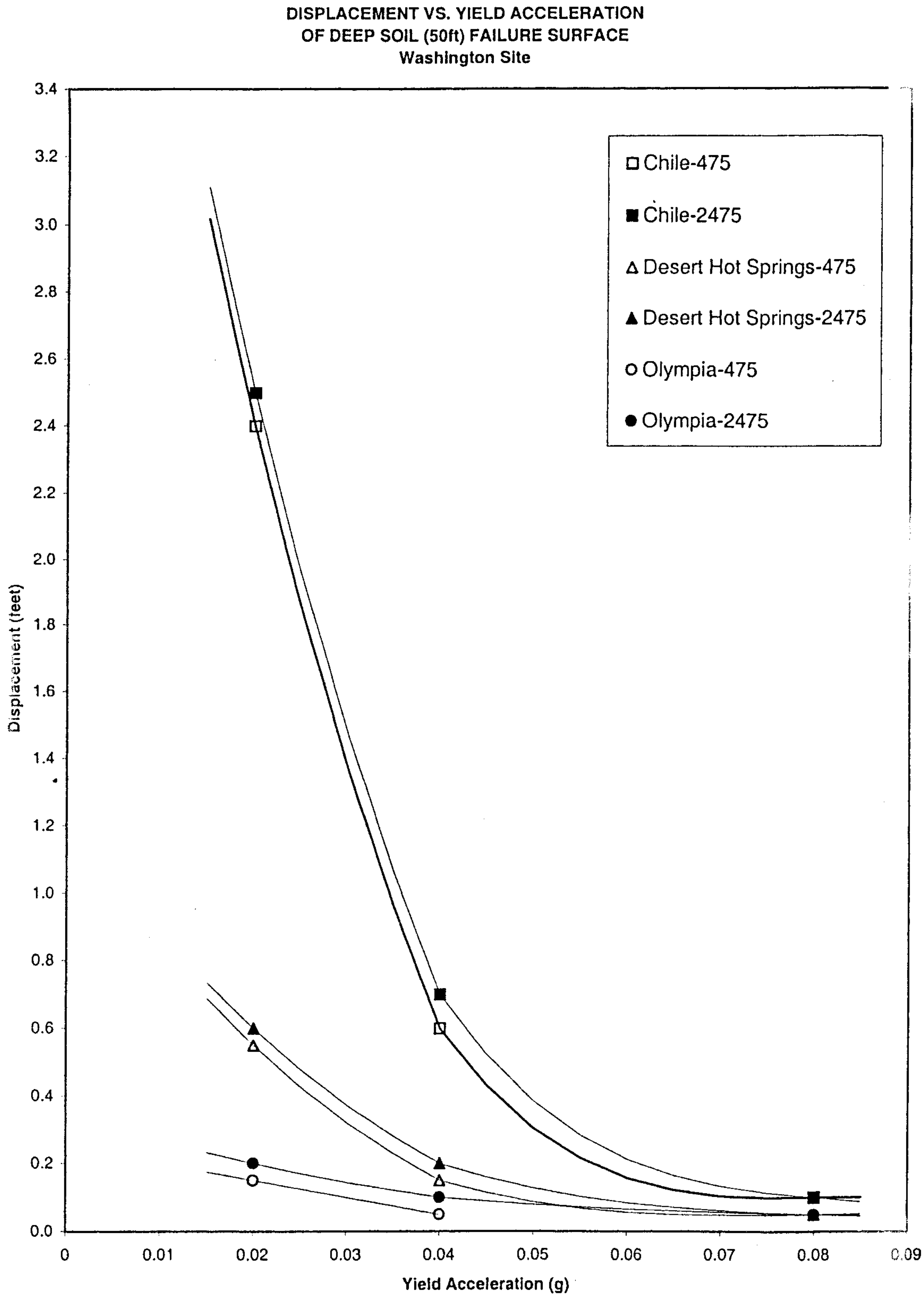

Figure H.13 Displacement vs. Yield Acceleration for the Deep Sliding Surface of the Western U.S. Site

This reaction force was introduced into the slope stability analysis using two methods:

1. A thin vertical slice the width of the pile group was placed at the location of the pile. This slice was assigned a strength that gives the same total pile resistance per unit width.

2. The resistance per unit width was converted into an equivalent shear strength along the shear plane in the liquefied zone, and this equivalent strength was added to the residual strength of 300 psf. For these analyses the upper failure plane was determined to be 104 feet in length giving an added component to the liquefied strength of 300 psf. The resulting strength assigned to the liquefied layer was 600 psf (i.e., 300 psf + 300 psf = 600). For the lower zone, the surface is 132 feet in length, resulting in an average pinning resistance of 530 psf and a total resistance of 830 psf.

Both procedures gave generally similar results.

The FOS for the lower surface is greater than 1.0 for the post-liquefaction case, indicating that a post-earthquake flow failure would not occur. However, under the slope inertial loading, displacement of the slope could develop, and this can be assessed using the Newmark sliding block analysis once the yield acceleration is determined. The upper surface has a FOS of 1.0, indicating that a flow failure is on the verge of occurring.

The yield acceleration for the lower surface was determined by varying the seismic coefficient within the slope stability analysis until the factor of safety was 1.0. This analysis resulted in the lower surface yield acceleration given below. For the upper surface, it was assumed that the yield acceleration was zero, since the FOS was 1.0 without any additional inertial force.

Case	Yield Acceleration (g)
Upper Surface	0
Lower Surface	0.02

For the ground improvement case different widths of improved ground were used below the abutment. The improved ground extended through each of the liquefied zones. Soil in the improved ground was assigned a friction angle of 45 degrees. This increase in strength was assumed to be characteristic of stone columns or a similar improvement procedure. As with the structural pinning case, two procedures were used to represent the improved zone. One was to model it explicitly; the second involved "smearing" the reaction from the improved strength zone across the failure surface by increasing the strength of the soil in the liquefied zone to give the same reaction. The resulting FOS was greater than 1.0 for all cases, indicating that flow would not occur. This allowed yield accelerations to be computed as a function of the width of the improved zone, in order to estimate the displacements that may occur. These values are summarized below.

Width (feet)	Yield Acceleration (g)
30	0.12
50	0.33
70	0.65

H.6.3.4 Displacement Estimates from Simplified Methods

Once lateral flow has been prevented, the amount of displacement that occurs from inertial loading on the failure wedge is estimated. This corresponds to Steps 3 and 11 of the design procedure.

Displacements were estimated for the yield accelerations given above using simplified methods. For these estimates, methods recommended by Franklin and Chang (1977), Hynes and Franklin (1984), Wong and Whitman (1990), and Martin and Qiu (1994) were used. All three methods approach the problem similarly. However, the Hynes and Franklin, as well as the Wong and Whitman and Martin and Qiu methods, eliminate some of the conservatism that is implicit to the Franklin and Chang method. For the Franklin and Chang method, it is necessary to define both the peak acceleration and velocity. The ratio of velocity to acceleration was assumed to be 30 for this study based on typical observations from recording of more distant events. For near-source events (epicentral distances less than about 15 km) this ratio can be as high as 60. In the case of the Hynes and Franklin method, displacements can be obtained for the mean, mean + 1σ, and upper bound displacements. The mean displacements are used for this study. The Martin and Qui study was based on the Hynes and Franklin database, but included the peak ground acceleration as an additional variable in the data regression analyses. Mean values were also used in their regressions. Each of these simplified methods relates displacement to the ratio of yield acceleration to the peak ground acceleration (k_{max}). For these evaluations k_{max} was 0.24g and 0.42g for the 10% PE in 50 and 3% PE in 75-year earthquakes, respectively. The resulting displacements for the cases cited above are summarized below.

It is the recommendation of the new provisions that a designer use the Martin and Qiu results. The Franklin and Chang, and Wong and Whitman, results provide possible upper and lower bound ranges on the displacements, but they are not believed to be as credible as the Hynes and Franklin, and Martin and Qiu, results.

Displacements (inches)				
	475-Year Event			
Case	F-C	H-F	W-W	M-Q
1	>36	16	10	28
2	<1	<4	<1	5
3	<1	<4	<1	<1
4	<1	<4	<1	<1
	2,475-Year Event			
Case	F-C	H-F	W-W	M-Q
1	>36	31	23	42
2	13	<4	3	8
3	<1	<4	<1	<1
4	<1	<4	<1	<1

Notes:

1: Pile Pinning/Lower
2: Stone Columns – 30 ft
3: Stone Columns – 50 ft
4: Stone Columns – 70 ft

The approximate displacement from the Martin and Qiu method for the 10% PE in 50 year is 28 inches. For the 3% PE in 75 year event the displacement is 42 inches. (See the table.)

H.6.3.5 Displacement Estimates Using Site Response Analysis Results

This section corresponds to Steps 3 and 11 of the design procedure, as they apply to site-specific analysis of potential displacements using the non-linear, effective stress method.

Similar estimates to the simplified methods described above may be made using the displacement versus yield acceleration curves shown in Figure H.13. As the curves are essentially identical for the 10% PE in 50 year and 3% PE in 75 year events, the displacement estimates shown in the table below are for both events and for the lower yield surface (45-55-foot depth).

Case	Displacements (inches)		
	Chile	Olympia	Desert Hot Springs
Pile Pinning	29	7	3
Stone Columns (> 30 foot width)	< 1	< 1	< 1

These estimates are generally consistent with the estimates from the simplified methods, although the site-specific results indicate that the event representative of the large mega-thrust subduction zone earthquake (Chile) will produce the largest displacements. The displacements from a moderate magnitude subduction zone intraslab earthquake (Olympia) and a moderate magnitude local shallow crustal earthquake (Desert Hot Springs) produce much more modest displacements that could be accommodated by the foundations.

H.7 STRUCTURAL ANALYSIS AND DESIGN

The design of bridge structures for liquefaction effects generally has two components. The first is that the bridge must perform adequately with just the liquefaction-induced soil changes. This means that the mechanical properties of the soil that may liquefy are changed to reflect their liquefied values (i.e., properties such as stiffness are reduced). Design for these cases is in reality a design for structural vibration effects, and these are the effects that the code-based procedures typically cover for design. The second component of the design is the consideration of liquefaction-induced ground

The potential interaction or combination of these effects must be addressed in the design, and at the present, there is not sufficient understanding of the phenomena to normally warrant performing a combined analysis. Therefore, the recommended methodology is to simply consider the two effects independently; i.e., de-coupled. The reasoning behind this is that it is not likely that the peak vibration response and the peak spreading or flow effect will occur simultaneously. In fact, for most earthquakes the peak vibration response is likely to occur somewhat in advance of the maximum ground movement loading. Furthermore, the de-coupling of response allows the flexibility to use separate and different performance criteria for design to accommodate the two phenomena. In some areas where extended shaking could result in the two phenomena occurring concurrently, it may be desirable to use more rigorous coupled effective stress computer models to evaluate this.

H.7.1 Vibration Design

Vibration design was done for both the AASHTO I-A Specifications and for the recommended LRFD provisions. For the recommended LRFD provisions, both the 3% PE in 75 year and 50% PE in 75 year events were considered. Since the primary objective of the study was to compare the existing and recommended provisions, the designs were more of a preliminary nature, which was felt to be sufficient to highlight the major differences. In this study, the same bridge was evaluated for each of the two specification requirements. Comparisons were then based on the amounts of reinforcing, for example, and in the case where sizes should be altered recommendations are given. To this end, the designs represent preliminary designs that highlight the differences between the two specifications. A very brief summary follows.

The bridge is comprised of multi-column bents so the existing provisions use an R-Factor of 5, and the recommended provisions allow an R-Factor of 6 provided a nonlinear static displacement check is done. For the 100 year design the proposed provisions allow an R of 1.3.

movements.

For the tallest columns and the recommended provisions, the 2,475-year event required a steel content in the columns of 1.4 percent, and this was controlled by the 100-year event. The 100-year event produced a design moment that was approximately 20 percent larger than the 2,475-year event. This is due to the relative magnitudes of R and of the input spectra. For the 475-year event a design using 1 percent steel resulted. For Pier 2 the results were similar.

The foundation (piling), used as starting point for both the existing and recommended provisions, was the same. This is because one objective of the study was to evaluate a system that worked for the existing provisions when subject to the effects of the larger design earthquake.

The pier designs were checked for displacement capacity, using an approximate push over analysis. The assessment considered the superstructure and the pile caps as rigid restraints against rotation for simplicity. While the check is only required for the recommended provisions, the checks were performed on the designs to the existing provisions, as well. All the columns met the checks (i.e., the displacement capacity exceeded the demands).

The recommended specification also requires that the displacements be checked for P- effects. In other words, the lateral shear capacity of the bents defines a maximum displacement that can occur without suffering problems from displacement amplification due to P- . Both piers are adequate as-designed with respect to P- .

H.7.2 Lateral Spreading Structural Design/Assessment

The material in this section generally represents Steps 4, 5, 6, 8, 9 and 12 of the Design Procedure, and the material addresses the structural aspects of the procedure.

In Article H.6.3 the tendency for the soil near Piers 5 and 6 to move during or after a major earthquake was assessed. Once it had been determined that lateral spreading would occur, the next step (Step 7) was to evaluate the beneficial pinning action of the foundation system in the analysis. This section describes the method of determining the pinning force to add to the stability analyses of Article H.6.3, and it describes the process of determining whether flow around the foundation would occur or whether the foundation will move with the soil. This involves Steps 4 and 5 of the design procedure.

H.7.2.1 Modes of Deformation

As outlined above there are two potential sliding surfaces during liquefaction for the Pier 5/6 end of the bridge. One is at the base of the upper liquefiable layer, and the other is at the base of the lower liquefiable layer. These potential deformation modes must be determined to evaluate the forces developed by the piles and the structures resistance.

The overall foundation deformation modes may be formally assessed using models that consider both the nonlinear nature of the soil resistance and the nonlinear behavior of the piles and foundations, when subject to prescribed soil displacement profiles. In this study, the deformations and structural behavior have been approximated using assumed displaced structural configurations that are approximately compatible with the constraints provided by the soil. Examples of these configurations are given in Figure D.4.4, D.4.5 and Figure H.14. In this example, the abutment foundation will move in a manner similar to that shown in Figure D.4.4, because there are sliding bearings at the substructure/superstructure interface. In the figure, the frictional forces transferred through these bearings have been conservatively ignored.

Pier 5 will move similar to the mode shown in Figure D.4.5. Under such a displaced shape both the columns and the piles contribute to the lateral resistance of the foundation. The columns contribute because there is an integral connection between them and the superstructure. In the current assessment, the residual displacements have been ignored. There exists some question as to whether this should be included or not. The reductions in resistance due to P- effects are likewise given in the figure, but for many of the deformations and column height combinations considered in this study, this reduction is small, and therefore it has not been included in the calculations.

H.7.2.2 Foundation Movement Assessment

As described in Step 4 through 6 of the design procedure, an assessment should be made whether the soil will move around the foundation or whether it will move the foundation as it moves. Passive capacities of the various layered soils were extracted from the p-y curves generated by conducting LPILE analyses[4] for the piles. These forces represent the maximum force that is exerted against the piles as the soil moves around the pile. This then is the upper bound limit state of the soil force that can be developed. Additionally, the maximum passive forces that can be developed against the pile caps and abutment stem wall were developed. Two total forces were developed; one for the shallow-seated soil failure and one for the deep failure. The shallow failure will develop approximately 1100 kips/pile and the deep failure approximately 3500 kips/pile at the point where the soil is moving around the foundation. By comparison, one pile with a clear distance of 30 feet between plastic hinges can develop about 90 kips of shear at the point where a full plastic mechanism has formed in the pile. The conclusion from this comparison is that there is no practical likelihood that the soil will move around the piles. Instead the foundations will be pushed along with the soil as it displaces toward the river channel beneath the bridge.

Intuitively, it is only reasonable to expect that soil will move around a pile if there is no crust of non-liquefied material being carried along with the displacing soil (Step 4 of the design procedure). In the case examined here, there are significant (10’s of feet) non-liquefied material above the liquefiable material, and it is that material which contributes to the high passive forces. Thus if a reasonable crust exists, the foundations are likely to move with the soil.

Now the questions to be considered are: 1) can the foundation systems endure the displacement that the soil produces (Step 6), and 2) can the foundations appreciably reduce the soil movement via pinning action (Step 7).

---

[4] LPILE is a computer program used to evaluate lateral response of piles subjected to loads and moments at the pile head. This program is similar to COM624.

H.7.2.3 Pinning Force Calculation

In Article H.6 various pinning forces were discussed and included with the stability analyses to investigate the effectiveness of including the existing foundation pinning. The following discussion accounts for the development of the force values used.

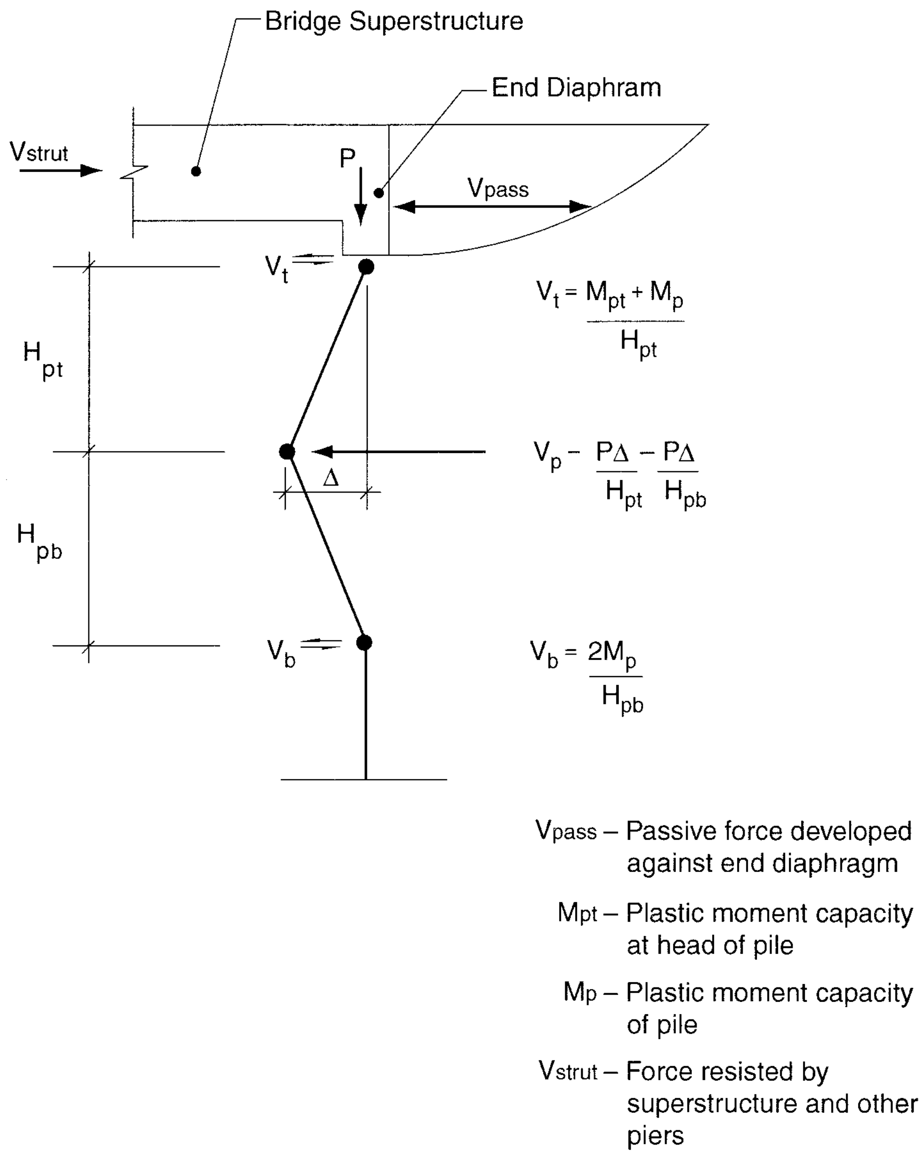

Figure H.14 Plastic Mechanism for an Integral Abutment Supported on Piles

Figure H.15 illustrates qualitatively the forces developed against the foundations and how they are reacted using the bridge, itself, as a strut. Two soil blocks are shown, Block A on the right and B on the left. Block A represents a postulated deep-seated slide that affects both Piers 5 and 6. The shears, V_{p5} and V_{p6}, represent the pinning shear force developed by the piles of Pier 5 and 6, respectively. Shear V_{c5} is the shear contributed by the Pier 5 columns. Finally, V_{pa5} is the passive resistance provided by the backfill acting against the end diaphragm.

While Block A is the most likely of the two to move, Block B is shown in this example to illustrate where and how the forces transferred into the bridge by Block A are resisted. In this case the bridge acts as a strut. Note that if a significant skew exists, then these forces cannot be resisted without some overall restraint to resist rotation of the bridge about a vertical axis.

Figure H.16 illustrates the pinning forces acting on a soil block sliding on the lower liquefiable layer. In this case, abutment and Pier 5 piles each contribute about 90 kips, the abutment about 400 kips, and the columns at Pier 5 about 420 kips. The total abutment pile resistance is 1080 kips and corresponds to the approximate plastic mechanism shear with 30 feet clear between points of assumed fixity in the piles. This comprises 10 feet of liquefiable material and 5D (D = pile diameter) to fixity above and below that layer[5]. The upper portion of the soil block is assumed to move essentially as a rigid body, and therefore the piles are assumed to be restrained by the integrity of this upper block. The pile resistance at Pier 5 is determined in a similar manner, and the shear that the Pier 5 piles contribute is 1440 kips. The abutment passive resistance corresponds to half of the prescribed passive capacity of the backfill and is assumed to act against the end diaphragm. The abutment fill is assumed to have slumped somewhat due to the movement of the soil block, and thus half of the nominal resistance was judged to be reasonable. The column resistance at Pier 5 is 420 kips, and this assumes that plastic hinging has occurred at the top and bottoms of the columns at this pier.

These forces (3360 kips) represent maximum values that occur only after significant plasticity develops. In the case of Pier 5 the approximate displacement limit is 22 inches, which comprises 4 inches to yield and 18 inches of plastic drift. The plastic drift limit is taken as 0.05 radians. The 22-inch displacement limit of Pier 5 is controlled by the piles. Because the piles of Pier 6 are the same, their limit is also 22 inches of displacement.

[5] Fixity was assumed to develop 5D above the liquefied layer. In an actual design case, a lateral analysis using a computer code such as LPILE could be conducted to be more rigorous about the distance to fixity.

Because the Pier 5 columns are longer than the distance between hinges of the piles, the column displacement limits are 34 inches total and 7 inches at yield. The fact that the piles control the displacement limit in this case implies that some margin is available in the column to accommodate any residual plastic hinge rotations that remain in the column after strong shaking stops.

Figure H.17 shows the displaced shape of the foundations for a shallow (upper layer) soil failure. In this case, the distance between plastic hinges in the piles is 30 feet, just as with the deeper failure, and thus the plastic shear per pile is 90 kips. The total contributed by the piles is 1080 kips as before.

In Article H.6.3, the estimated displacements for the lower or deeper failure wedge were 28 inches for the 10% PE in 50 year event and 42 inches for the 3% PE in 75 year event. Neither of these are within the plastic capacity of the piles and either additional piles could be added as ‘pinch’ piles or ground remediation could be used[6]. It will be recalled that the yield acceleration for the upper failure was essentially zero for both the 10% PE in 50 year and 3% PE in 75 year events, which indicates that some remediation would be required to stabilize the fill and its toe for both design events.

H.8 COMPARISON OF REMEDIATION ALTERNATIVES

The primary intent of these analyses was to determine the potential effects of increasing the seismic design criteria from its current probability of exceedance from 10% in 50 years to a 3% in 75 years. Liquefaction was predicted for both return periods, and as a consequence, there is little difference in what remedial work is required for the two return periods.

H.8.1 Summary of Structural and Geotechnical Options

Mitigation measures are assessed based on the desired performance requirement of the bridge. The first option is to assess the performance in its as-designed configuration. If this results in

[6] Pinch piles refer to piles driven at close spacing to increase the shear resistance or density of a soil mass. In the Pacific Northwest, these piles are often timber.

unacceptable performance, a range of mitigation measures is assessed.

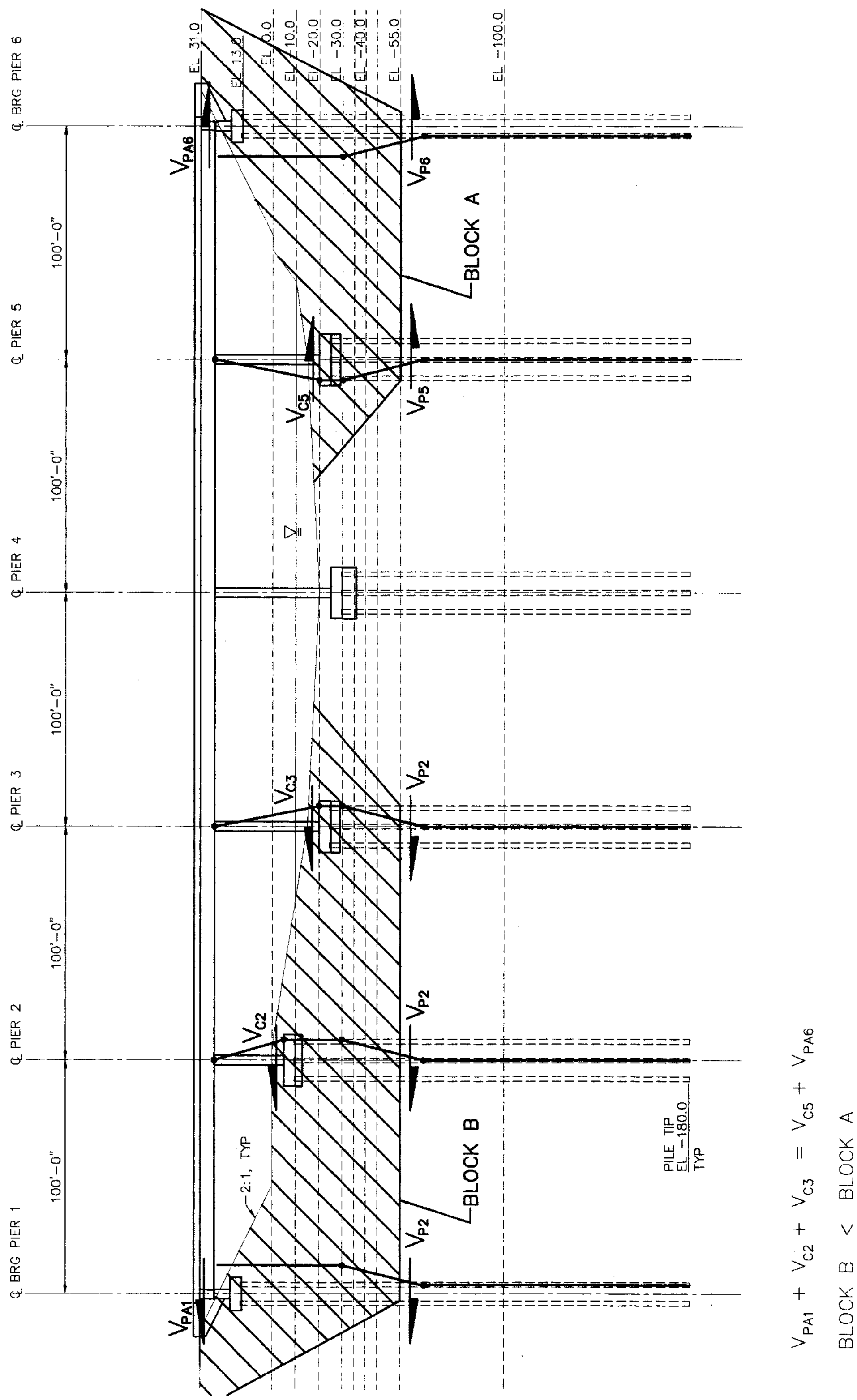

Figure H.15 Forces Provided by Bridge and Foundation Piling for Resisting Lateral Spreading

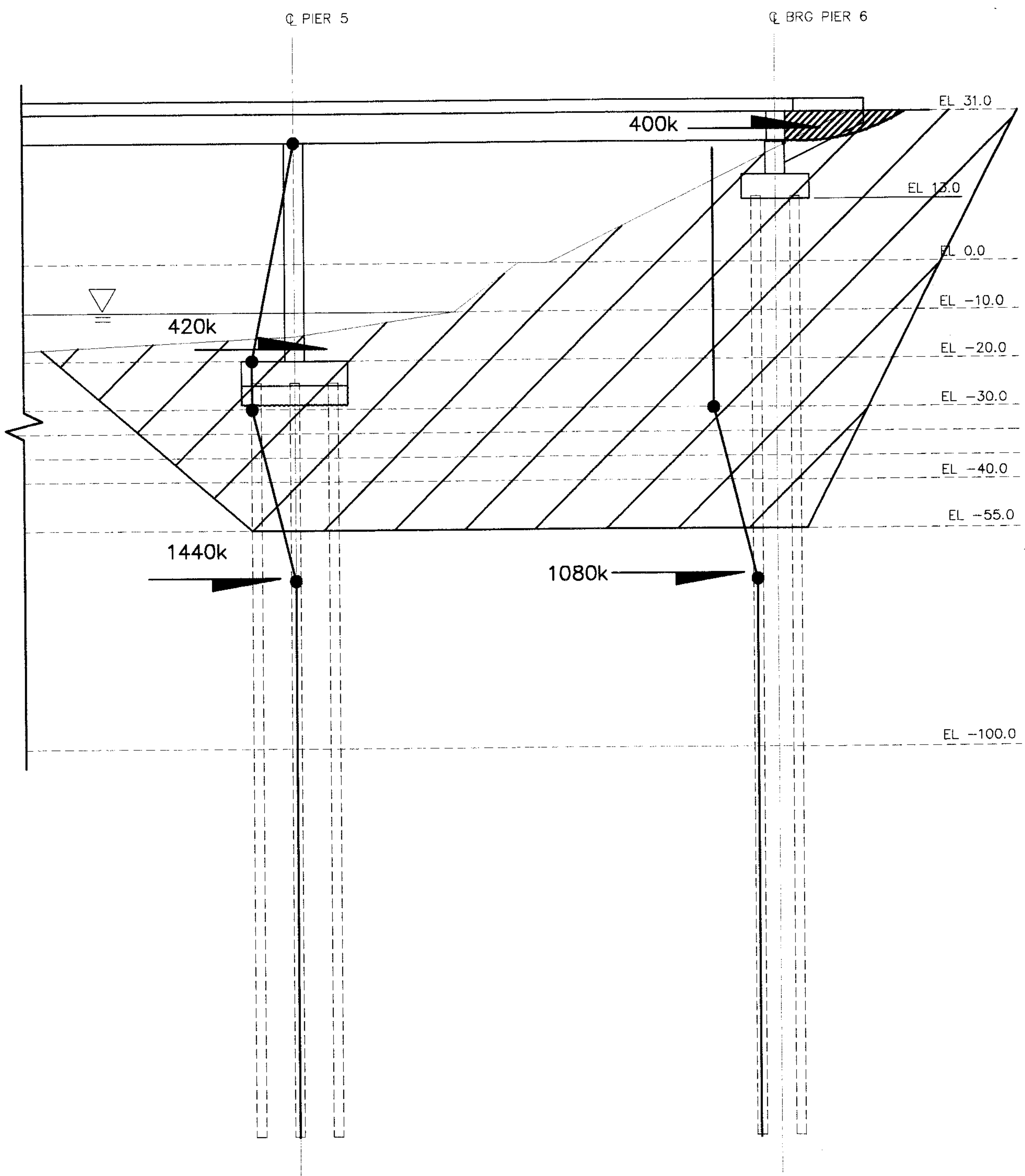

Figure H.16 Piers 5 and 6 Resisting Lateral Spreading – Deep Wedge

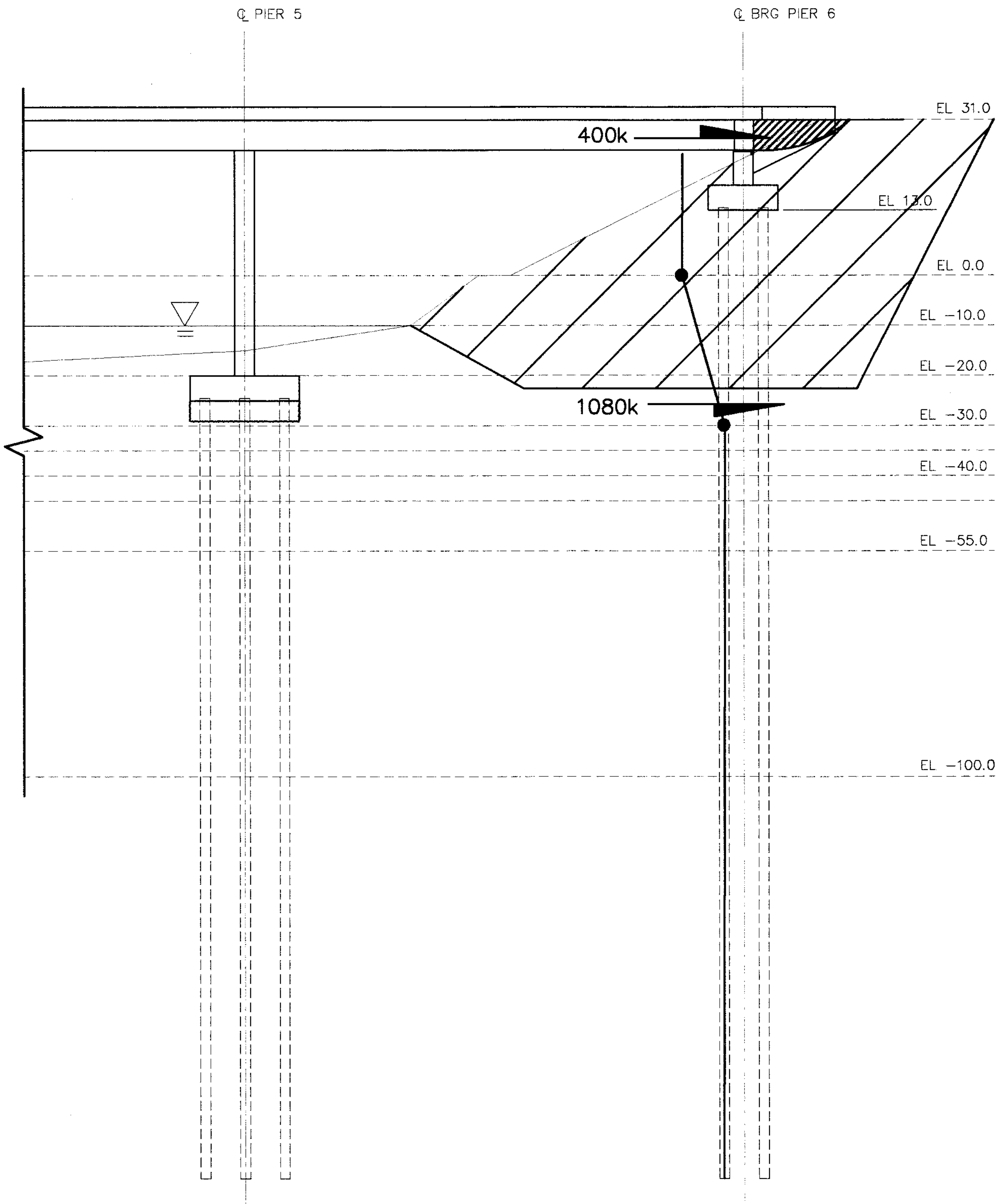

Figure H.17 Pier 6 Resisting Lateral Spreading – Shallow Wedge

For this example, some form of structural or geotechnical remediation is required at the right-hand abutment because the yield acceleration for the upper failure wedge is zero. This implies that this wedge is unstable under static conditions after the soil liquefies, which it does in both the 3% PE in 75 year event and 10% in 50 year event[7]. Two choices for improving the conditions were considered - use of additional piles or stone columns. Since the yield acceleration for the upper failure surface is so low, the more effective choice of the two was to use stone columns. These provide the combined advantage of increasing the residual shear strength of the sliding interface, and they can reduce pore water pressure build up, thereby postponing or possibly eliminating the onset of liquefaction.

Because the lower failure wedge also has a relatively low yield acceleration, 0.02 g, it makes sense to extend the mitigation deep enough to improve the deeper soil layers, as well. This low yield acceleration results in displacements of 28 inches and 42 inches for the 10% PE in 50 year and 3% in 75 year events from the simplified analyses and displacements of approximately 29 inches for both events for the time history corresponding to the mega thrust subduction zone earthquake for the site-specific Newmark analyses. The decision to improve the deeper layers requires that stone columns extend on the order of 50 feet in depth. The stone column remediation work will provide displacements that are less than 4 inches. This will keep the piles within their elastic range, and this will meet the highest level of operational performance objectives in the foundation system.

Although in this example the left-hand abutment was not evaluated in detail because the FOS of the initial stability analyses was greater than 1, a cost/benefit assessment would typically be made to determine if some remediation work on the left-hand abutment would be cost effective. Once a contractor is mobilized on the site, it would make some sense to provide improvement on both sides of the river. It may be that upon more in-depth investigation the stone columns could be spaced further apart or applied over a smaller width on the left-hand bank.

[7] The approach fill and ground profile condition for the bridge considered in this study are more severe than that used in the actual bridge that this example was modeled after. Thus, the implication of instability here does not imply instability in the prototype structure.

H.8.2 Comparisons of Costs

As noted above, the remedial work is required for both the 10% PE in 50 year and 3% PE in 75 year events.

The stone column option would likely be applied over a 30-foot length (longitudinal direction of bridge), since that length produced acceptable deflections of less than 4 inches for the site specific results, which is within the elastic capacity of the piles. The width at a minimum would be 50 feet, and the depth also would be about 50 feet. If the columns were spaced roughly on 7-foot centers, then 40 stone columns would be required. At approximately \$30 per lineal foot (plf), the overall cost per approach fill would be on the order of \$60,000, or about \$120,000 for both sides if the left-hand fill were judged to require remediation.

As a rough estimate of the cost of the overall structure, based on square-footage costs of \$100 to \$150 in Washington, the bridge would cost between 2 and 3 million dollars. If the higher cost were used, due to the fact that the bridge is over water and the foundation system is relatively expensive because of its depth, the cost to install stone columns on the right-hand side would run about 2% of the overall cost of the bridge. If both sides were remediated, then the costs would comprise about 4% of the bridge costs. It should be noted that this additional cost will produce a foundation performance level that meets the operational criteria for both return period events.

If pinch piles were used to augment the piles of the foundations, the pinch piles would not need to be connected to the foundation, and they would not need to extend as deep as the load-bearing foundation piles. The per pile costs for the foundation piles were estimated to be on the order of \$10,000 to \$12,000 each for 180-foot long piles. If shorter piles on the order of 80-feet long were used, their costs would be about half as much. Thus if pinch piles were used about 10 to 12 piles per side could be installed for the same cost as the stone column remediation option. Although detailed analyses have not been performed with these pinch piles, the amount of movement anticipated would be in the range of 6 to 12 inches, rather than the 4 inches obtained with the stone columns. Therefore, the stone column option would appear the more cost effective in this situation. On a specific project, combinations of the two options would be evaluated in more depth.

It is useful to recognize that in this situation some remediation would be required for both the 10% PE in 50 year and 3% PE in 75 year events because of the predicted instability of the upper failure wedge. In the case of the former, the remediation is required to a depth of 50 feet because the anticipated movement of the lower failure wedge would be on the order of 28 inches for the simplified analyses and 30 inches for the site specific analysis and thus be in excess of the 22 inch limit. For the 3% PE in 75 year event, movement on the order of 42 inches is predicted by the simplified analysis, and 30 inches by the site-specific analyses. Consequently, remediation is required to a depth of 50 feet for both events. Hence the difference in cost for this site and bridge between the two design earthquakes is minimal.

H.9 MISSOURI EXAMPLE

The second bridge considered in this study is located in the New Madrid earthquake source zone in the lower southeast corner of Missouri. This general location was selected because this zone is one where a significant seismic hazard occurs, and there are numerous stream crossings and low-lying areas where potential for liquefaction also exists. Additionally, the project team wished to include a non-western site where the effects of different source mechanisms and where the differences in shaking levels between the 475-year and 2,475-year events would be highlighted. Since the design process and procedures used for this example are the same as the Washington example, an abbreviated summary of the key results follows. The details of the work on this bridge can be found in NCHRP 12-49 Liquefaction Report.

H.9.1 Site Characterization and Bridge Type

The site is located in southeastern Missouri along the western edge of the Mississippi River alluvial plane near the New Madrid seismic zone. Soils at this site consist of 20 feet of clay over a 20-foot layer of sand over dense alluvial materials at depths greater than 40 feet. The Missouri Department of Transportation (MoDOT) provided site characterization information for the prototype site, including boring logs with SPT's, CPT soundings, and shear wave velocity data. The geotechnical information was collected by MoDOT for a lifeline earthquake evaluation that they are currently conducting.

The simplified bridge used for the over-crossing is approximately 180 feet long, and comprises three, roughly equal-length spans. There are no horizontal or vertical curves on the bridge, and the bridge has no skew. A general elevation of the bridge and of the ground line is given in Figure H.18 (Fig 4.3). The bridge and site plan have been simplified from that initially provided by MoDOT for illustrative purposes. The configuration of the bridge was selected, in part, due its common nature. Many states use this type of bridge or variations to this type of bridge. Thus it was felt that the results for such a bridge type would be widely relevant to many other regions around the country.

The bridge structure comprises AASHTO prestressed girders supported on three-column bents. The roadway is approximately 38 feet wide, and five 39-inch girders with a concrete deck form the superstructure. The substructure is formed of 3-foot diameter columns, which support a 40-inch dropped cap-beam. The foundations of the intermediate piers are individual pile caps for each column that are supported on 14-inch steel pipe pile foundations. An elevation of one of the intermediate piers is given in Figure H.19.

The abutments are of the integral type, where the end diaphragm is integrated with the ends of the girders and deck and is directly supported by nine 14-inch-diameter pipe piles. These piles form a single line in the transverse direction to the bridge. An elevation of the abutment is shown in Figure H.20.

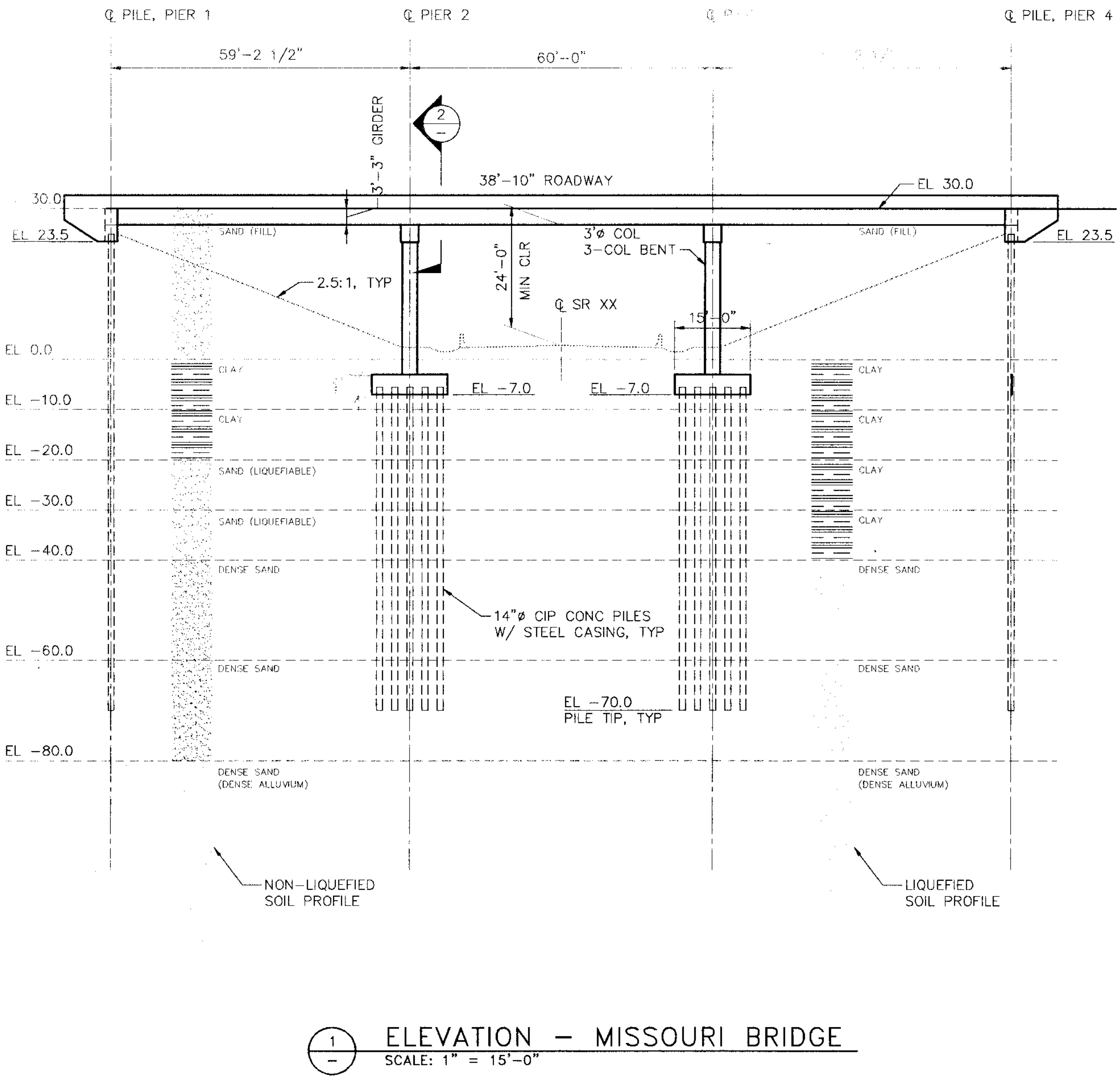

Figure H.18 Elevation and Ground Profile for the Mid-America Bridge

The deaggregation results for the Missouri site show that, for both 475-year and 2,475-year return periods and for both short periods and long periods of the response spectrum, the ground motion hazard is dominated by magnitude 8 earthquakes occurring 30 to 80 km from the site. These earthquakes are associated with the New Madrid seismic zone. The range of distances from the New Madrid source reflects the modeling by USGS of the earthquake fault(s) within a relatively broad source zone, since the exact location of the fault(s) within the zone are not known.

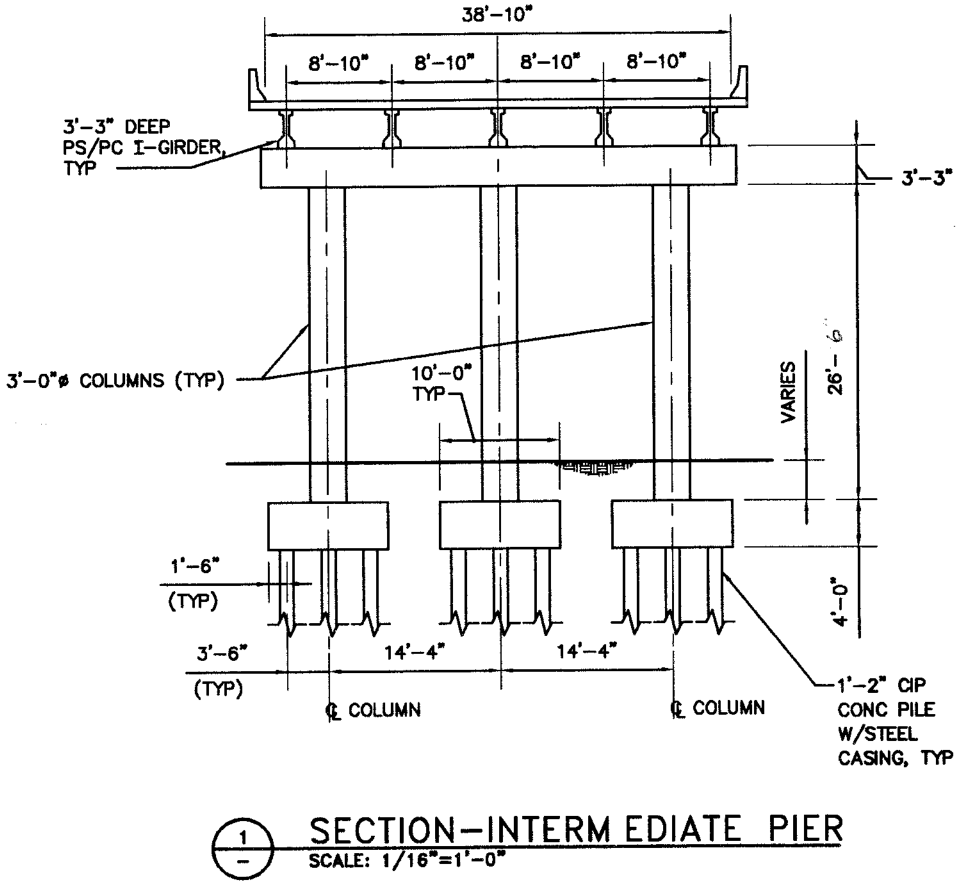

Figure H.19 Elevation of Intermediate Pier

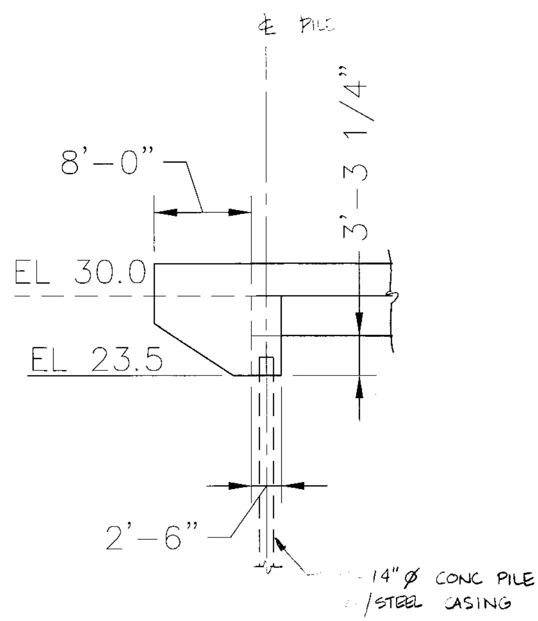

Figure H.20 Elevation of Integral Abutment

The deaggregation results for the Missouri site differ from the results for the Washington site, where three different seismic source types and magnitude and distance ranges contributed significantly to the ground motion hazard. For the Missouri site a single large magnitude source mechanism dominates the seismic hazard. Three natural recordings were selected from large magnitude earthquakes in Mexico, Chile and Japan to represent the time domain characteristics of the design earthquakes. These records were frequency scaled to be consistent with the design spectra for the site.

H.9.2 Liquefaction Analyses

The first step of the procedure outlined in Article D.4.2.2 is to determine if liquefaction occurs.

Simplified liquefaction analyses were conducted using the procedures given in Youd and Idriss (1997). Two levels of peak ground acceleration (PGA) were used, one representing the 475-year event within the current AASHTO Specification and the other representing the recommended 2,475-year event. The PGA for the 475-year event was not adjusted for site effects, consistent with the approach recommended in the AASHTO Standard Specifications[8]. Ground motions for the 2,475-year event were adjusted to Site Class D, using the procedures given in Section 3 of the recommended LRFD provisions. The resulting PGA values for each case are summarized below.

Input Parameter	475-Year Return Period	2,475-Year Return Period
Peak ground acceleration	0.17g	0.53g
Mean Magnitude	6.6	7.5

The magnitude of the design earthquake is required for the SPT and CPT simplified analyses. As discussed previously, results of deaggregation studies from the USGS database for deaggregation suggest that the mean magnitudes for the 475- and 2,475-year events are 6.6 and 7.5, respectively. The mean magnitudes reflect contributions from small to moderate magnitude earthquakes occurring closer to the site. However, the dominant event is the characteristic magnitude 8 earthquake in the New Madrid seismic zone. For the simplified liquefaction assessment, a range of magnitudes thought to be representative of practice was used in the evaluation. For time history analyses, acceleration time histories representative of the duration of the Magnitude 8 New Madrid earthquake and the levels of ground motion defined by the current AASHTO spectrum and the MCE spectrum of the recommended specification were developed.

For these analyses ground water was assumed to occur 20 feet below the ground surface for the non-fill case.

Factors of safety (FOS) results from the liquefaction evaluations for the simplified soil model without fill for the three magnitudes are shown in Figure H.21 and Figure H.22 for the 475-year and 2,475-year seismic events, respectively. These results indicate that liquefaction may or may not occur for the smaller event, depending on the assumed magnitude of the earthquake. For the magnitude based on the mean of the deaggregation for the site, liquefaction is not predicted. For the 2,475-year event, liquefaction is predicted, regardless of the assumed magnitude.

Ground response analyses were also conducted using DESRA-MUSC, similar to those described in Section H.6.2. Results of these analyses are included in the NCHRP 12-49 Liquefaction Study (2000). Based on the simplified liquefaction analyses and on the nonlinear effective stress modeling, it was concluded that lateral spread deformations would be distributed over the 20- to 40-foot depth. However, for analysis purposes, in order to compute likely displacement magnitudes of the overlying 20 feet of clay and embankment fill, it was assumed that ground accelerations, at the 40 feet interface depth would control the displacement, assuming a Newark sliding block analogy.

[8] Common practice is to adjust the PGA for the site factors given in Table 2 of Division 1-A. While this adjustment may be intuitively correct, these site factors are not explicitly applied to the PGA. If the site coefficient were applied at the Missouri site, the PGA would be increased by a factor of 1.5, reducing the difference in the ground motions between the 475 year and the 2475 year events.

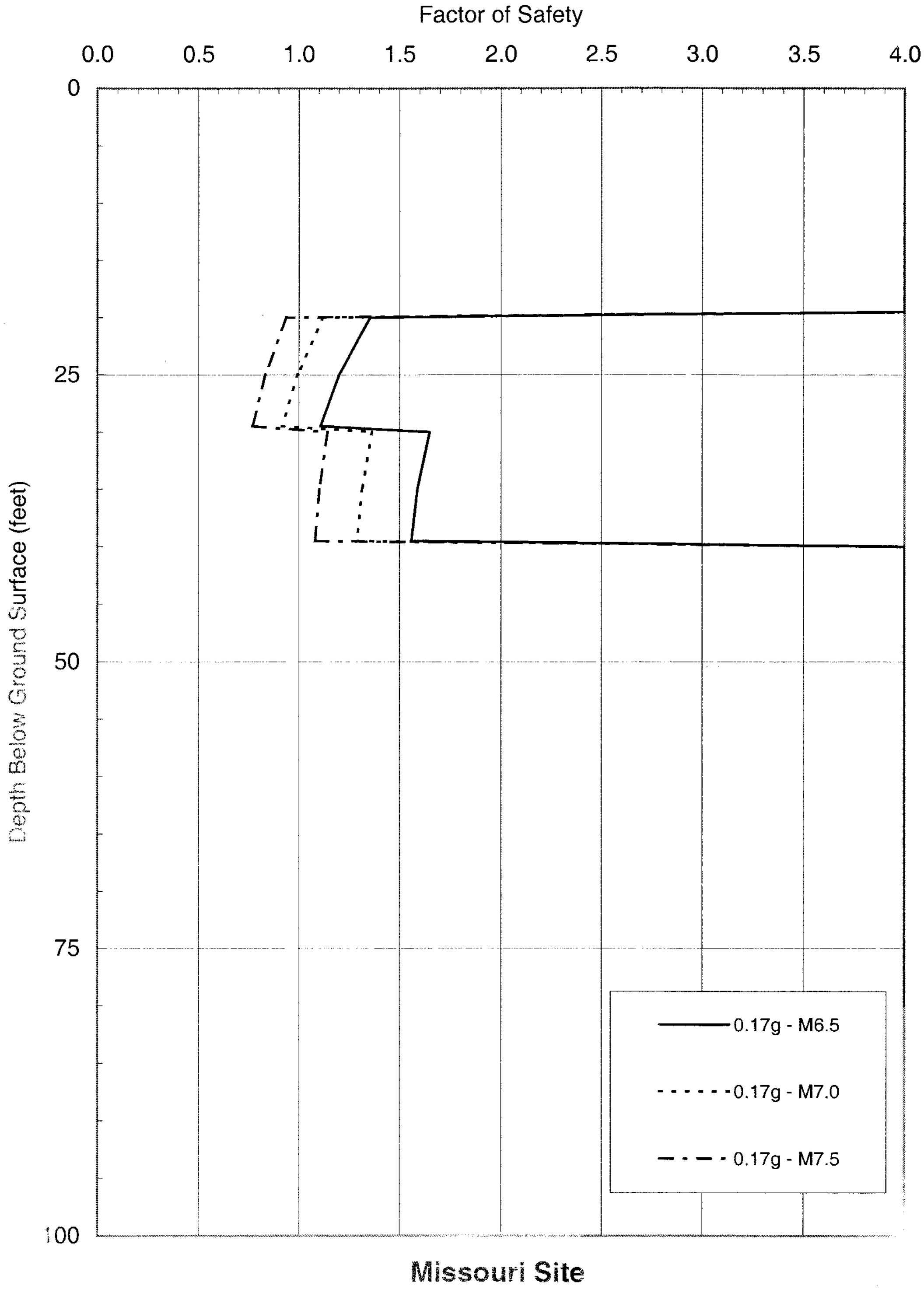

Figure H.21 Liquefaction Potential – 475-Year Return Period

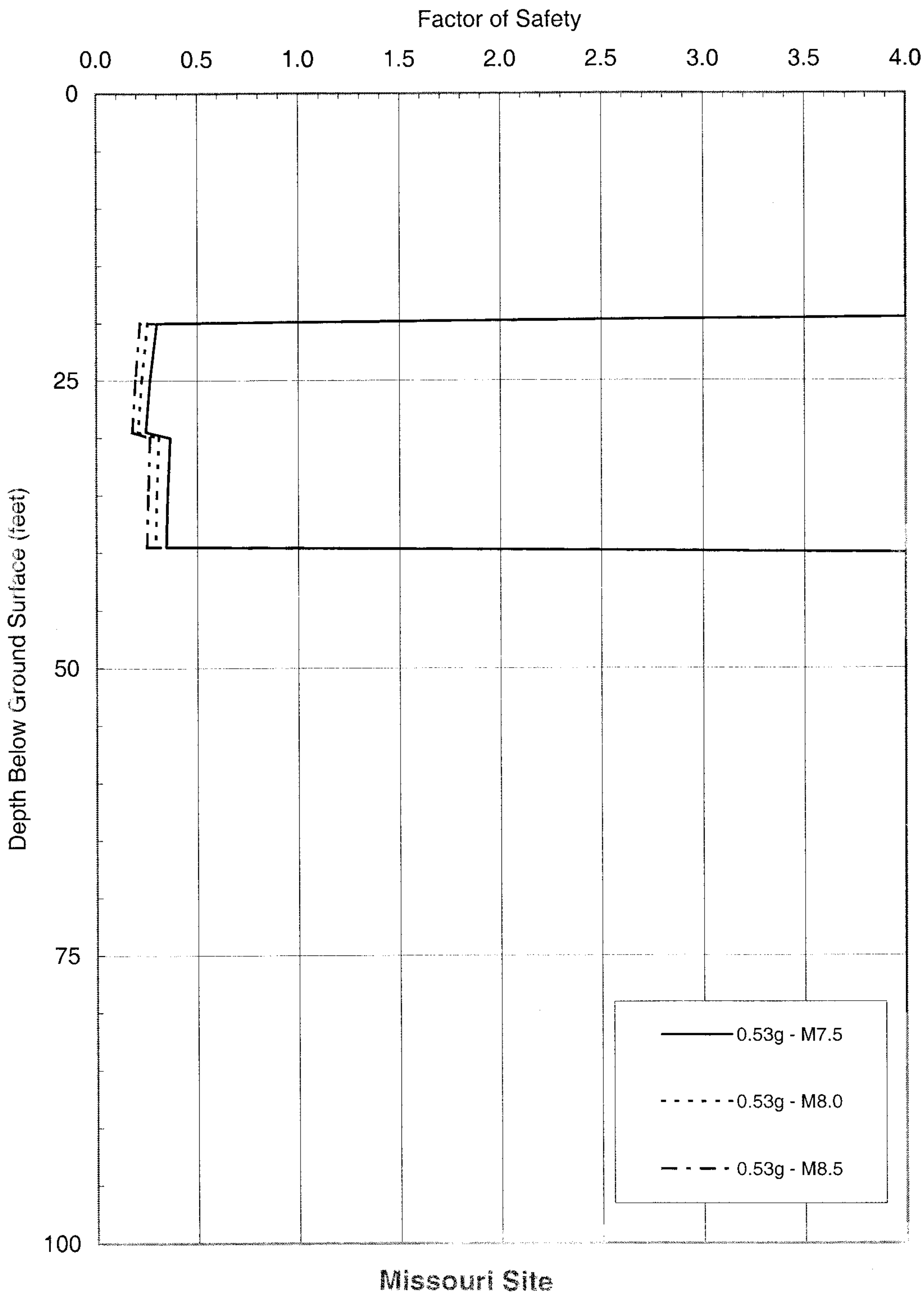

Figure H.22 Liquefaction Potential – 2,475-Year Return Period

H.9.3 Initial Stability Analysis

The first step in the liquefaction evaluation involved an analysis of the post-earthquake stability. In this analysis stability was evaluated for the liquefied condition but without a seismic coefficient. This check was performed to determine if a flow failure would occur in the liquefied state. Results from these analyses show that the FOS dropped significantly when a residual strength was assigned to the liquefied layer; however, the FOS was greater than 1.0, indicating that a flow failure was not expected. This allowed displacements to be estimated using the simplified Newmark method described previously in Article H9.2.

Yield accelerations were initially estimated without consideration of the pinning effects of piles by re-running the stability analyses for the liquefied soil profile, with different applied seismic coefficients. The yield acceleration from these analyses is the inertial force required to produce a FOS of 1 and was determined to be approximately 0.02. Displacements were estimated using the same methods and assumptions as presented for the Washington site, except that the peak ground acceleration and the yield acceleration were those for the Missouri site. The displacements determined for the two return periods are summarized at the table below.

Case: End Slope Displacements (inches)			
F-C	**H-F**	**W-W**	**M-Q**
475-Year Event:			
>36	>10	5	5
2,475-Year Event:			
>36	28	32	32

In these analyses, methods proposed by Franklin and Chang (1977), Hynes and Franklin (1984), Wong and Whitman (1990), and Martin and Qiu (1994) were evaluated. The provisions recommend that mitigation decisions be based on the results from the Martin and Qiu (M-Q) simplified method, which give results of 5 inches and 32 inches for the 475- and 2,475-year events, respectively. These displacements are large enough, particularly for the 2,475-year event, that some mitigation procedures would have to be considered. These mitigation methods could involve structural pinning or ground improvement as described in the next section.

As for the WSDOT site, analyses were also performed using the DISPMNT computer program in combination with DESRA-MUSC results. "Upslope" deformations were suppressed assuming a strong one directional driving force from the embankment. Strengths on the interface were degraded as a function of pore water pressure increases for the 35-40 foot layer, and reduced to the 300 psf residual strength when liquefaction was triggered. Results showing displacement time history plots for the 2,475-year Michoacan earthquake as a function of yield acceleration are shown Figure H.23. The input acceleration time histories used at a depth of 40 feet (70 feet with 30 feet of fill) are shown in Figure H.24. The time histories are very similar for the no fill and fill cases. Total accumulated displacements for all earthquake events are shown in Figure H.25, where it may be seen that the 2,475-year events generated significantly larger displacements than 475-year events, at low values of yield acceleration. These displacements were used as a basis for discussion of remediation analyses, as described in Article H.9.4.

Similar displacement estimates to the simplified methods described above, may be made using the displacement versus yield acceleration curves shown in Figure H.25. The free field displacements without mitigation corresponding to a yield acceleration of 0.02 are summarized below:

Case: End Slope		
Displacement (inches)		
M	**C**	**T-O**
475-year event:		
21	21	16
2,475 year event:		
180	150	140

Notes:

M, Michoacan earthquake
C, Chile earthquake
T-O, Tokaji – Oki earthquake

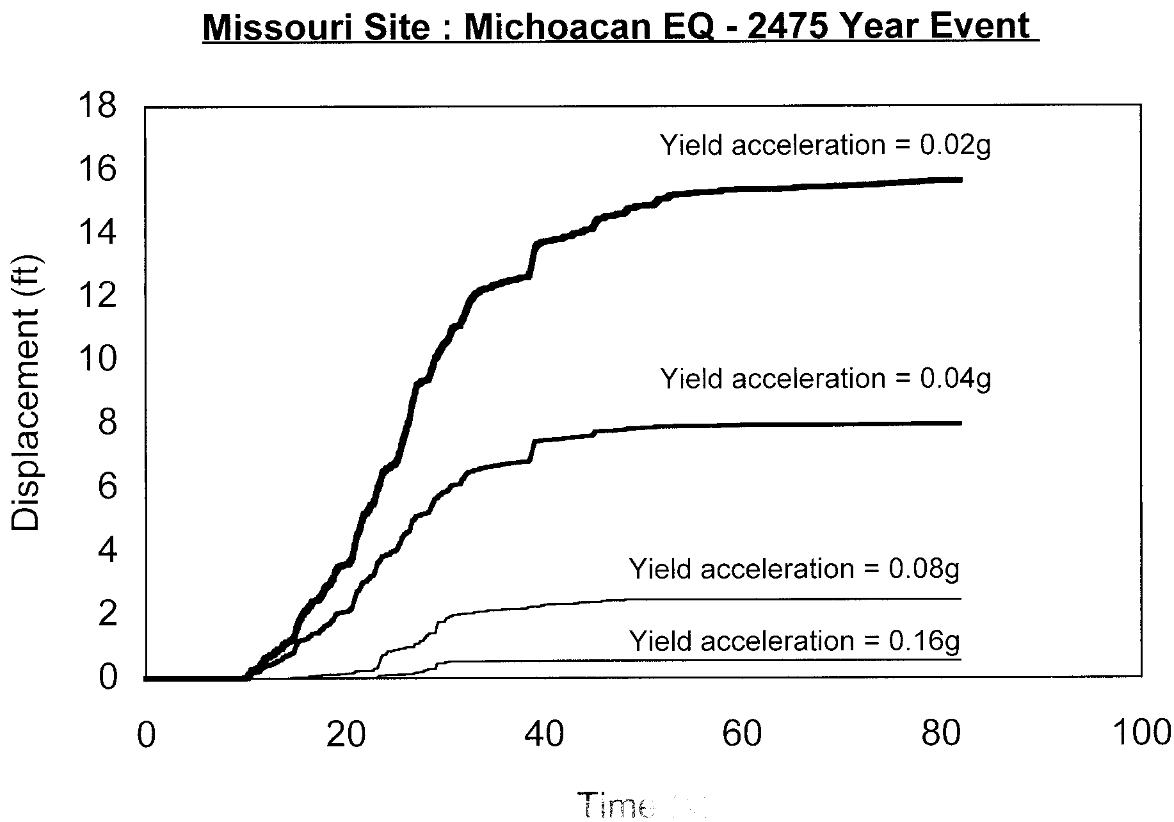

Figure H.23 Displacement vs. Time for the Mid-America Site Failure Surface

H.9.4 Stability Analyses with Mitigation Measures

Two procedures were evaluated for reducing the amount of displacement being predicted - structural pinning and ground improvement. For these analyses the additional resistance provided by the improved ground or by the structural pinning of the soil was incorporated into the stability analyses as described previously.

For the structural pinning evaluation, shear forces were calculated for two cases. In the first case, the shear failure occurred at the toe of the end slope in front of Pier 3 (Figure H.26). This gave an increase in resistance of 16 kip/foot for the 43-foot width of the abutment. Both pile pinning and abutment passive resistance are included in this reaction. This reaction occurs over the 35-foot abutment width, resulting in a resistance of 33 to 44 kips/foot of width. This reaction force was introduced into the slope stability analysis using the smearing method described for the Washington study. For this method the resistance per unit width was converted into an equivalent shear strength along the shear plane in the liquefied zone and this equivalent strength was added to the residual strength of 300 psf. For these analyses the failure plane was determined to be 90 feet in length giving an added component to the liquefied strength of 180 psf. The resulting strength assigned to the liquefied layer was 480 psf (i.e., 180 psf + 300 psf = 480 psf).

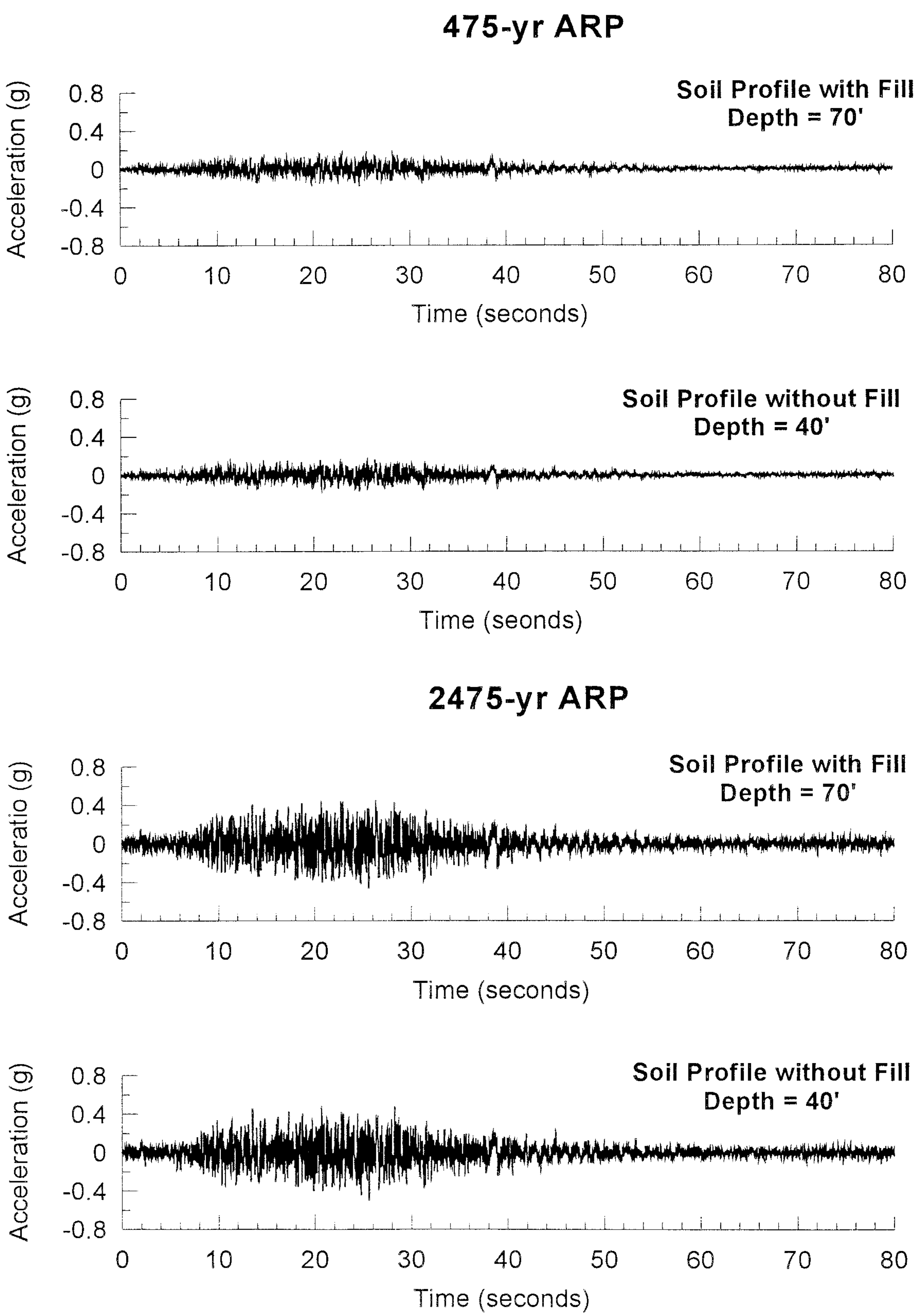

Figure H.24 Input Acceleration History at Base of Liquefiable Layer, 1985 Michoacan EQ

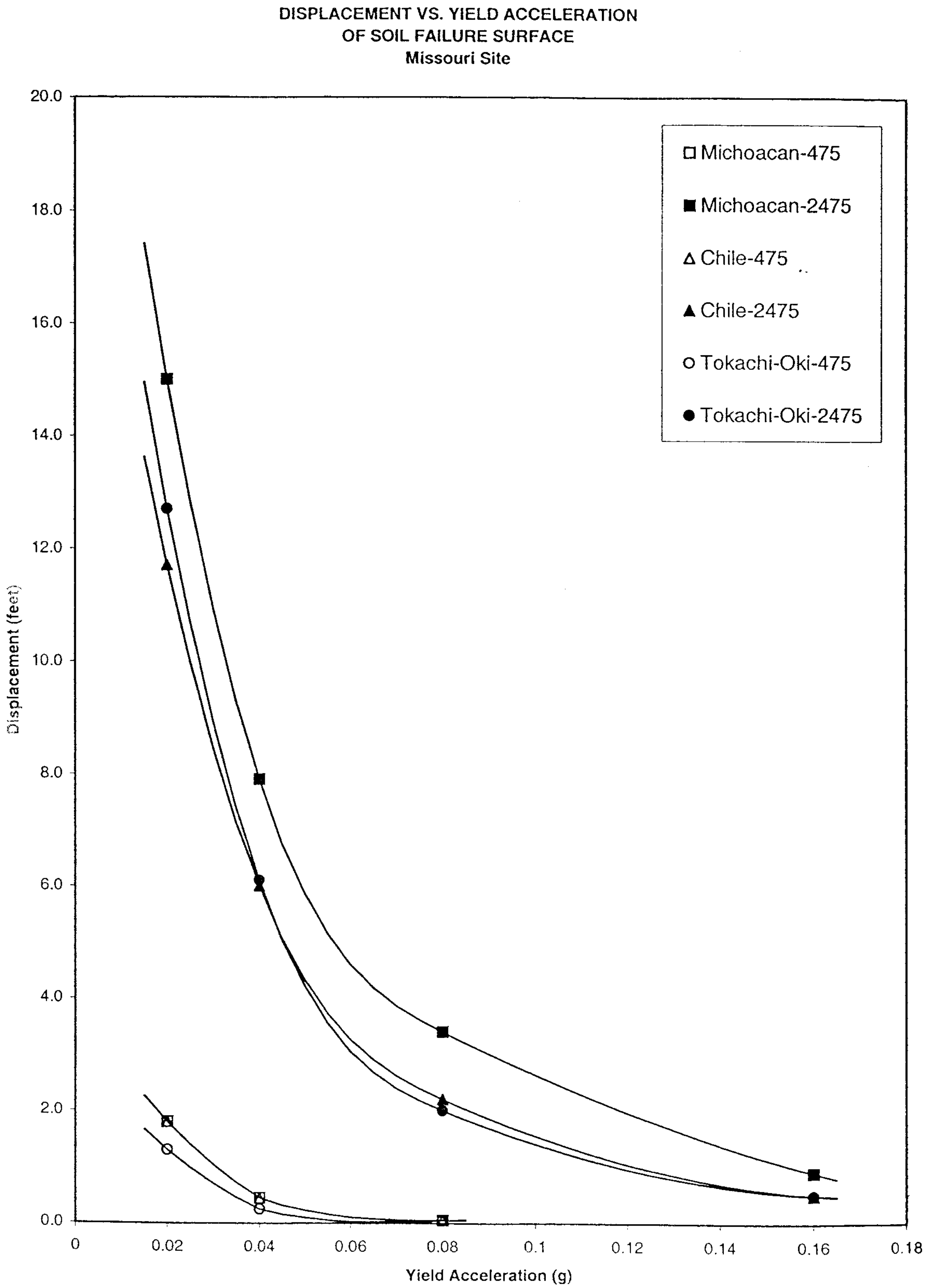

Figure H.25 **Displacement vs. Yield Acceleration of the Soil Failure Surface for the Mid-America Site**

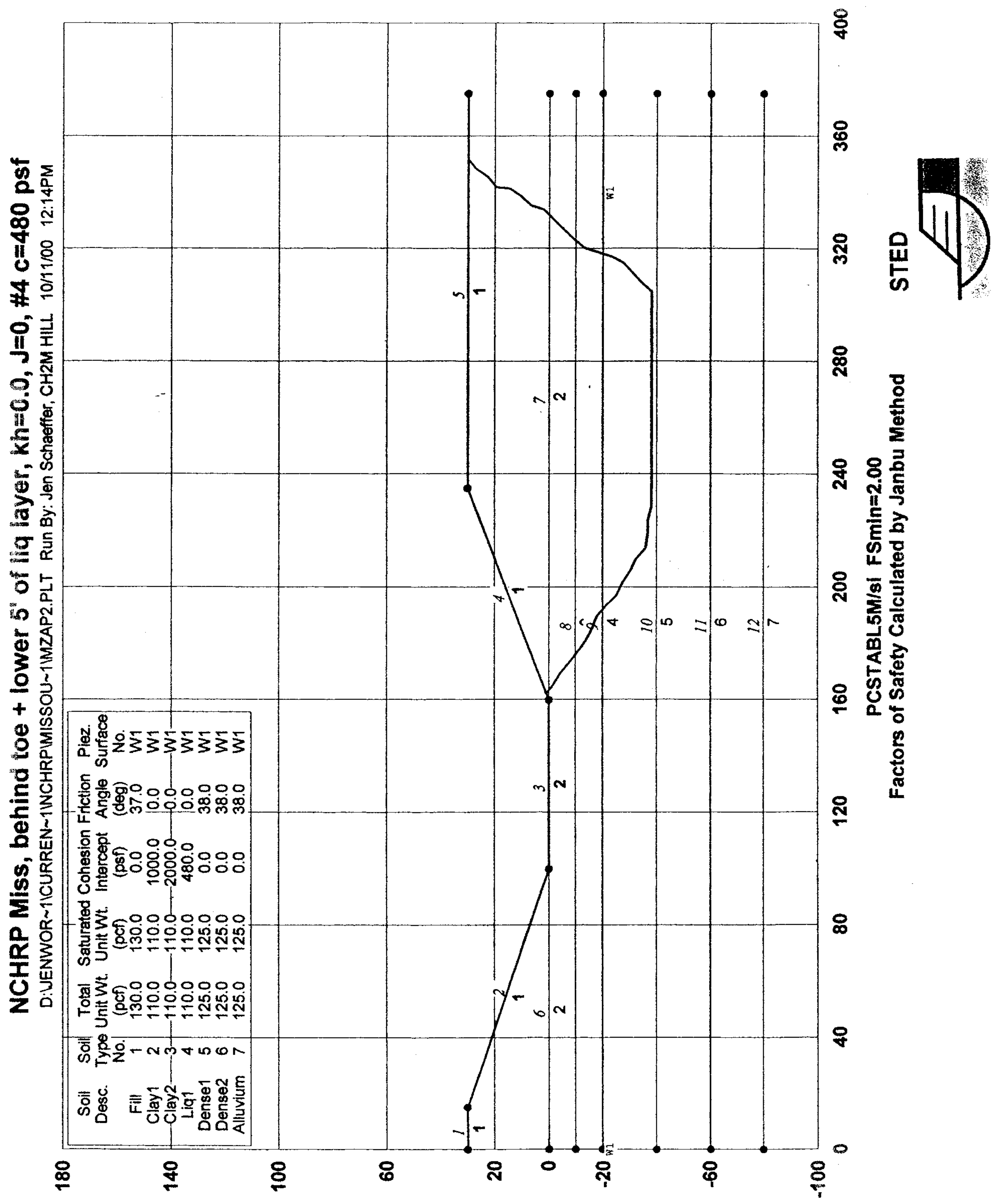

Figure H.26 Geometry of Toe Failure Wedge for Missouri Site

For the second case, the shear failure was allowed to extend to the opposite embankment, as shown in Figure H.27. The pinning force for this case was 32 kip/foot, resulting in an additional 355 psf of smeared resistance. The resulting assigned strength for the layer was 655 psf (i.e., 355 psf + 300 psf = 655 psf).

Yield accelerations for both cases were determined by varying the seismic coefficient within the slope stability analysis until the factor of safety was 1.0. This analysis gave the following yield accelerations for the two cases.

Case	Yield Acceleration (g)
Toe Wedge	0.12
Deep Wedge	0.10

For the ground improvement case different widths of improved ground were used below the abutment. The improved ground extended through each of the liquefied zones. Soil in the improved ground was assigned a friction angle of 45 degrees. This increase in strength was assumed to be characteristic of stone columns or a similar improvement procedure. As with the ground improvement studies for the Washington site, two procedures were used to represent the improved zone. One was to model it explicitly[9]; the second involved "smearing" the reaction from the improved strength zone across the failure surface by increasing the strength of the soil in the liquefied zone to give the same reaction. The resulting FOS was greater than 1.0 for all cases. This allowed yield accelerations to be computed as a function of the width of the improved zone. These values are summarized below.

Width (feet)	Yield Acceleration (g)
10	0.18
30	0.33
50	0.53

[9] The "explicit" case involve modeling the geometry of the correct width of improved ground in the computer. While fundamentally more correct, it is also time consuming to change the geometry of the problem for each width. The smearing technique involved a simple change in strength of the soil layer, which could be accomplished very quickly.

H.9.5 Displacement Estimates from Simplified Methods

Displacements were estimated for each of the yield accelerations given above. In these analyses methods recommended by Franklin and Chang (1977), Hynes and Franklin (1984), Wong and Whitman (1990), and Martin and Qiu (1994) were used. The same assumptions as made for the Washington site were used during these analyses. The resulting displacements for the cases cited above are summarized below.

Displacements (inches)				
475-Year Event:				
Case	**F-C**	**H-F**	**W-W**	**M-Q**
1	<1	<4	<1	<1
2	<1	<4	<1	<1
3	<1	<4	<1	<1
4	<1	<4	<1	<1
5	<1	<4	<1	<1
2,475-Year Event:				
Case	**F-C**	**H-F**	**W-W**	**M-Q**
1	>36	<4	5	3
2	>36	5	8	5
3	8	<4	2	1
4	<1	<4	<1	1
5	<1	<4	<1	<1

Notes:

1: Toe Wedge
2: Deep Wedge
3: Stone Columns – 10 ft
4: Stone Columns – 30 ft
5: Stone Columns – 50 ft

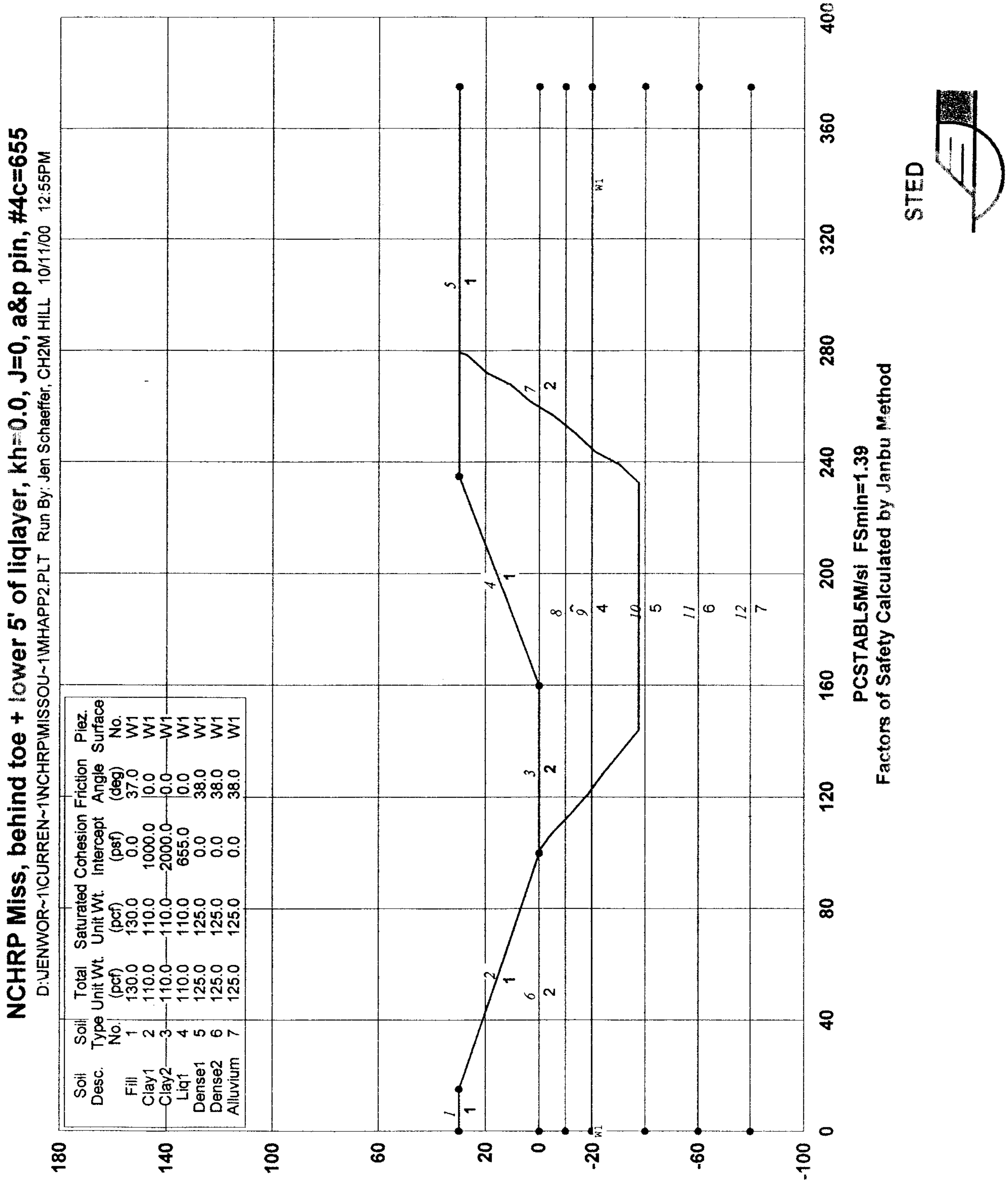

Figure H.27 **Geometry of Deep Failure Wedge for Missouri Site**

The estimates for the recommended Martin and Qui method indicate that for the 475-year event the displacements will be <1 inch for both the toe and deep wedge cases. For the 2,475-year event, the toe wedge case gives 3 inches and the deep wedge 5 inches. Virtually any pinning or ground improvement method will limit displacements to less than about 0.5 feet for the 2,475-year event. (Putting aside the F-C displacements, which are based on a limited database and also reflect an upper bound.)

Similar displacement estimates to the simplified methods described above, may be made using the displacement versus yield acceleration curves shown in Figure H.25. The free field displacements without mitigation corresponding to a yield acceleration of 0.02 are summarized in Article H.9.4.

For the pile pinning and ground remediation yield accelerations described in Article 9.4, the displacement estimates are summarized below:

Displacements (inches):			
	M	**C**	**T-O**
Case	**475-Year Event:**		
1	<1	<1	<1
2	<1	<1	<1
3	<1	<1	<1
4	<1	<1	<1
5	<1	<1	<1
	2,475-Year Event:		
Case	**M**	**C**	**T-O**
1	24	12	12
2	30	18	18
3	6	4	4
4	<1	<1	<1
5	<1	<1	<1

Notes:

M, Michoacan earthquake
C, Chile earthquake
T-O = Tokaji – Oki earthquake
1: Toe Wedge
2: Deep Wedge
3: Stone Column – 10 ft
4: Stone Column – 30 ft
5: Stone Column – 50 ft

For the 2,475 earthquake events, the displacements tabulated above are in general less than the Franklin and Chang estimates but higher than the Hynes and Franklin and the Wong & Whitman and Martin and Qiu estimates.

H.9.6 Pinning Force Calculations

As with the Washington study, the soil movements will induce forces in the superstructure, if either the toe wedge or the deep soil wedge failure develops. The toe wedge only involves the abutment for pinning force, whereas the deep wedge involves both Pier 3 and the abutment. Additionally, the same potential failure modes exist for the left-hand end of the bridge, but since the bridge is symmetric the results for one end apply to the other.

Figure H.28 illustrates the pinning forces acting on the soil block comprising the toe wedge. In this case, the nine piles contribute 105 kips at the bottom of the slide, and they contribute 53 kips at the top. The top force is smaller than the bottom because the top is assumed to be a pinned condition. The location of the central plastic hinge is taken at mid-height of the soil column. The abutment backwall also contributes lateral force that resists the movement of the toe wedge, and that resistance is 520 kips, which is half that available typically. The reduction is taken to recognize the potential for slumping of the backfill due to movement of the toe wedge of soil.

These forces represent maximum values that only occur after significant plasticity develops. In the case of the piles, about 7 to 8 inches of lateral movement occurs at the center plastic hinge shown in the figure before full yield is attained. Subsequent to yielding the maximum deflection that can tolerated with 0.05 radians of plastic drift is 18 inches. This is the maximum total structural deflection allowed for the toe wedge movement.

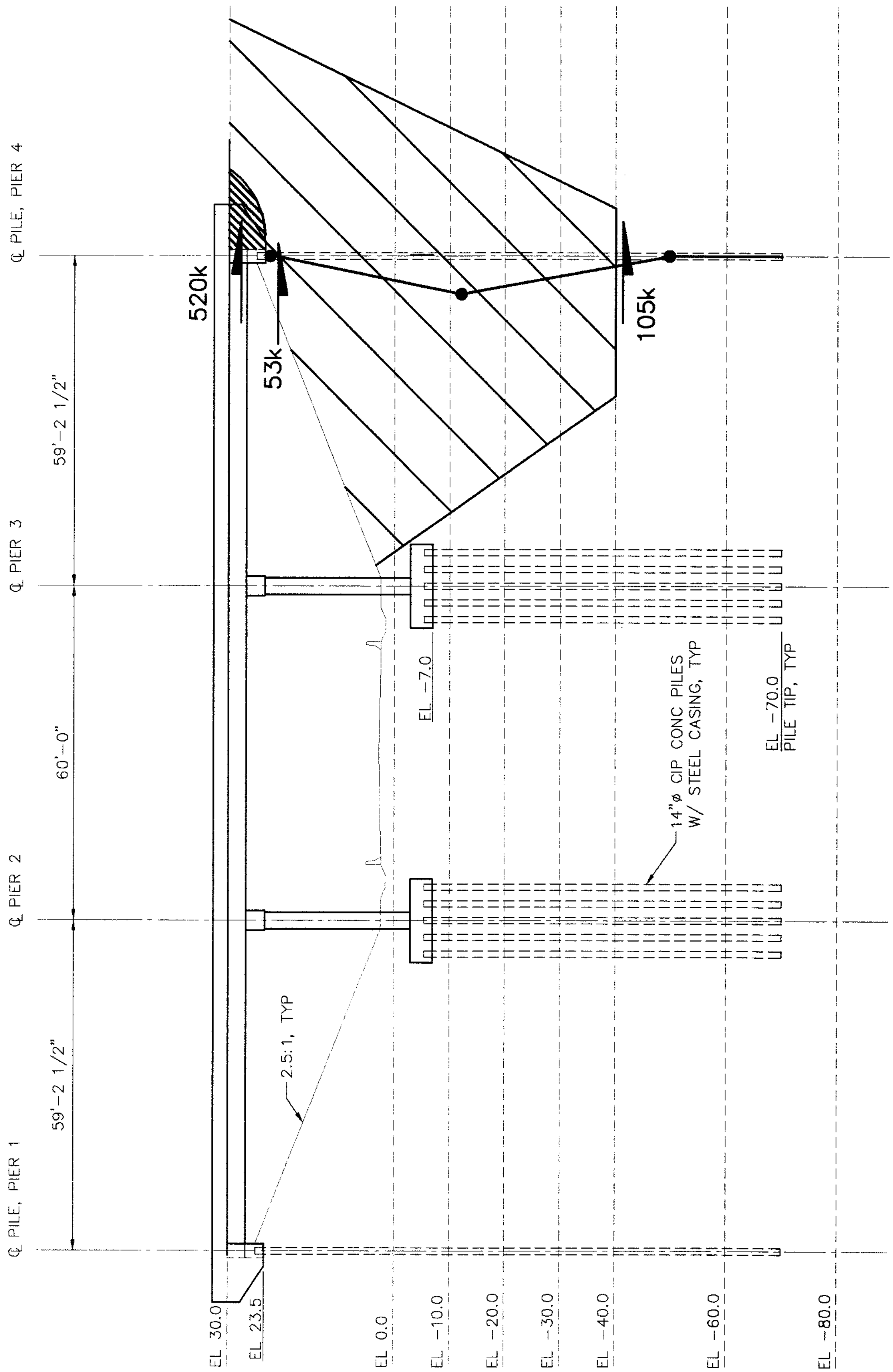

Figure H.28 Pier 4 Structural Forces Resisting Lateral Spreading

Figure H.29 shows the displaced shape when the deep wedge of soil moves. This involves the abutment piles and Pier 3. For the abutment the same resistances and allowable deformations apply as with the toe wedge failure addressed above. For Pier 3 the piles can develop 531 kips of resistance, based on plastic hinges forming 5D above and below the liquefiable layer. This results in about 32 feet of length between plastic hinges in the piles. Additionally, the columns contribute 166 kips to the resistance. The bent was assumed to be connected to the superstructure with a pin connection. This is a reasonable bound for the common details used to connect girder superstructures, provided a full-depth diaphragm is used. The connection typically then behaves as a 'piano hinge'.

The allowable displacements for the deeper wedge failure are approximately 24 inches, which represents total displacement. Pier 3 develops yield at about 6 inches and then can tolerate roughly 18 inches of plastic deformation. However, because both the abutment piles and Pier 3 are moved by the deep wedge, the 18 inch total displacement allowed at the abutment controls. Therefore 18 inches is the allowable displacement.

In Section H.9.5 the estimated deformations for the 475-year event are 7 inches for the deep wedge failure and 5 inches for the toe wedge failure. For the 2,475-year event, including the pinning effect of the substructure, produces displacements of 11 and 14 inches for the toe and deep wedge failures, respectively. This is just in excess of the yield displacements for the piles, but is within their 18-inch plastic capacity, and is thus judged acceptable. This illustrates the potential beneficial effect of considering pinning.

The site-specific predictions of ground motion are given in Figure H.30, and at a yield acceleration of about 0.1g, which applies for the pinning options, the average displacement of the three time histories is about 20 inches. In this case, the site-specific data produces displacements (due mainly to the Michoacan earthquake record) that exceed the simplified methods' predictions, but are close to the plastic capacity of the piles.

The conclusion is that if one wished to be conservative and use the results of the site-specific analysis and not risk displacements close to the capacity of the piles, then some remediation would be desirable to protect the substructure. However, if one used the simplified methods for estimating displacements, then the structure, as designed could withstand the 2,475-year event and the liquefaction that it induces, and the piles would be just beyond their elastic capacity. This range in predicted displacements illustrates the uncertainty associated with the prediction of ground movements.

H.9.7 Comparison of Remediation Alternatives

As with the study of the Washington bridge, the intent of the Missouri study was to assess the potential consequences of changing the AASHTO seismic design provisions. This comparison met the objectives by having little if any liquefaction under the 475-year event and large amounts of liquefaction and associated ground movements during the 2,475-year event. It is clear that the structure, as designed, is capable of resisting the lateral spreading associated with the liquefaction without the need for any additional expenditure of funds.

Because the estimated performance under the 2,475-year event produces spreading displacements that will exceed the elastic capacity of the piles, it was worthwhile to investigate mitigation measures that would produce higher levels of performance, so that the piles can remain within their elastic capacity.

Stone columns can be used to limit the displacement of the toe and deep soil wedges. In Section H.9.5 , 10-foot, 30-foot, and 50-foot wide buttresses of stone columns were considered. The calculated displacements were all less than about 4 inches for the 2,475-year event when the stone columns were employed, and this provides the operational performance level for the foundations. This displacement ensures the piles remain within their yield displacement.

It is evident that mitigation, if it is deemed necessary to meet higher performance levels, is only required for the 2,475-year event. All the displacements for the 475-year event, when pinning is considered, are acceptable.

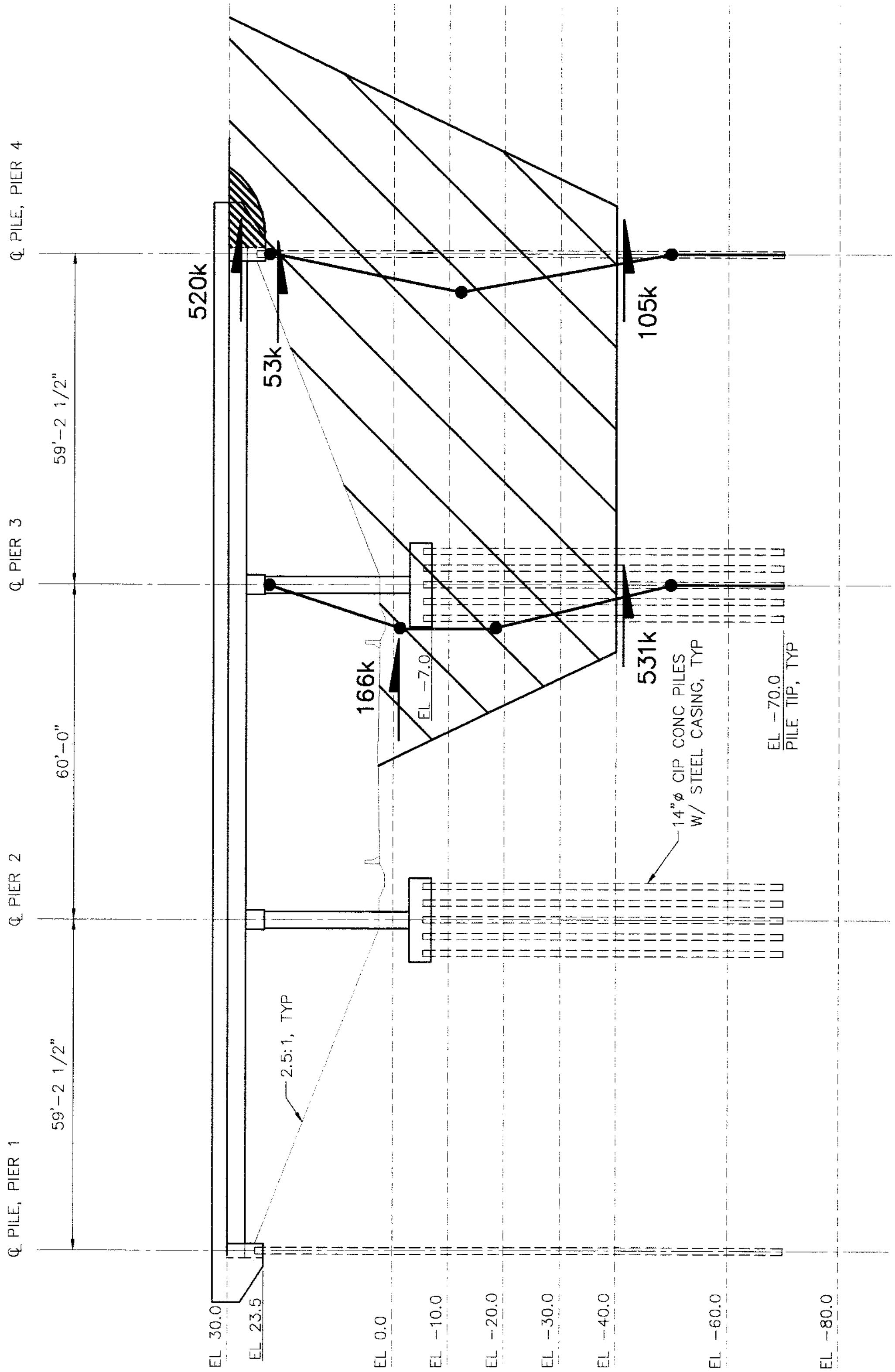

Figure H.29 Pier 3 and Pier 4 Structural Forces Resisting Lateral Spreading

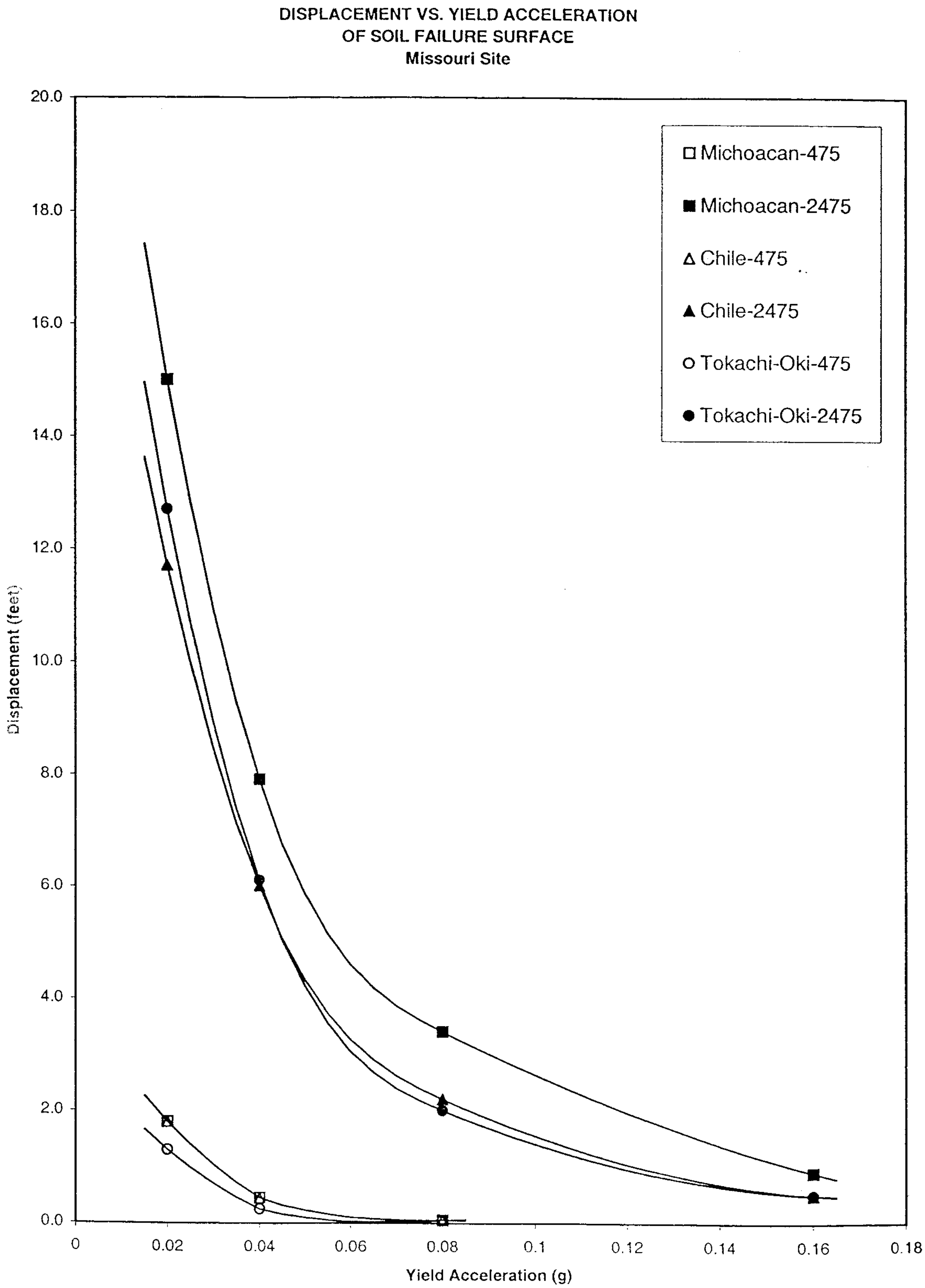

Figure H.30 Displacement vs. Yield Acceleration of the Soil Failure Surface for the Mid-America Site

If additional piles are considered for limiting the overall soil displacements, then the objective would likely be to install enough to reduce the estimated displacements down to values that would be tolerable for the substructure. This would likely require a large number of piles since the existing restraint at the superstructure level currently provides over 50% of the pinning resistance. Thus the inference is that if the deformations need to be limited beyond that which the foundation pinning alone can produce, then stone columns appears to be the rational choice.

There are no additional costs necessary in order to meet the life-safety performance requirements of the 2,475-year event. In this example, spreading displacements of the order of less than 14 inches would be estimated, and these can be accommodated in the piles. If a higher level of performance is desired, such that the piles remain within their elastic limits and spreading displacements are desired to be less than 4 inches, then some remediation work is necessary for the 2,475-year event.

The stone column option would likely only need to be applied over a 10-foot length (longitudinal direction of bridge), since that length produced acceptable deflections of 4 inches or less in the Newmark analysis. The width at a minimum would be 50 feet, and the depth also would be about 40 feet. If the columns were spaced roughly on 7-foot centers (the width would grow to 14 feet), then about 20 stone columns would be required. At approximately $30 plf, the overall cost per abutment would be on the order of $24,000 or about $50,000 for both abutments.

As a rough estimate of the cost of the overall structure, based on square-footage costs of $80 to $100, the bridge would cost between about $600,000 and $800,000. Thus, the cost to install stone columns would run about 6 to 8 percent of the overall cost of the bridge. This expenditure would ensure the highest operational level of performance of the structure because foundation movements would be less than the yield level of the piles.

If pinch piles were used to augment the piles of the foundations, the piles would not need to be connected to the foundation, and they would not need to extend as deep as the load-bearing foundation piles. The per pile costs for the foundation piles were estimated to be on the order of $2500 each for 70-foot long piles. If shorter piles on the order of 40-feet long were used, their costs would be roughly $1500 each. Thus if pinch piles were used, about 15 piles per side could be installed for the same cost as the stone column remediation option. It is not likely that this number of piles would be as effective in limiting soil movement as the stone columns, although they would produce an acceptable level of performance. Therefore, the stone column option would appear the most cost effective in this situation.

H.10 SUMMARY AND CONCLUSIONS

These recommendations apply when liquefaction at a site has been determined to be likely as a result of the 2,475-year earthquake. The specific criteria are given in Section 3.10.5 of the recommended LRFD provisions.

There are two phenomena that must be considered in the design of a bridge on a liquefiable site. The first is the traditional vibration design based effectively on the response spectra for the site. This corresponds to the design cases dealt with in the current AASHTO Division I-A. The second phenomenon is lateral forces induced by flow sliding or lateral spreading if these potential consequences of liquefaction are predicted to occur. Flow sliding describes the condition where a soil mass is statically unstable after liquefaction-induced weakening of the soil occurs. Such an unstable condition can lead to quite large deformations. Lateral spreading describes deformations that progressively occur during ground shaking due to the combined static plus transient inertial forces exceeding the resistance of the liquefied soil. Deformations due to lateral spreading typically are smaller than those due to flow sliding.

For the MCE event, when the recommended performance objective is life-safety, inelastic deformation is allowed in the foundation for the lateral spreading or flow spreading case. Mitigation measures are able to achieve higher levels of performance when desired, so that piles remain within their elastic capacity. The vibration cases are designed, as they always are, for inelastic response above ground and at inspectable locations. It is believed that allowing some inelastic action in the presence of large spreading movements during the MCE is necessary. Because spreading-induced deformations are 'displacement –controlled', instability of the system is unlikely even though some damage may exist in the foundations. The implication of this decision is that a bridge and its foundations may need to be replaced after a MCE event, but it avoids a significant expenditure of funds to prevent the displacement from occurring.

The design for vibration and lateral spreading is split into two independent activities, as coupling of the vibration load case and the spreading load case is not usually warranted. The vibration design is considered separately from the spreading design, because it is unlikely that the maximum vibration effect and the maximum lateral spreading forces occur simultaneously. The de-coupled approach is considered reasonable with respect to the current state of the art.

The approach recommended is to determine the likely ground movements that may occur at the site, including the effects of altered site configurations such as fills and the beneficial effects of the pinning of piles. This prediction of lateral spreading can be made using either currently accepted simplified methods or site-specific analyses, as outlined in this report. As noted in the two cases studied, there can be a significant variation in the predicted displacements using the different methods, and this indicates that a designer must be aware that there can be a significant range in anticipated movements. Refined accuracy is not warranted. The beneficial resistance of the substructure should be included in the assessment of movements. The substructure is then assessed for the predicted movements, and if it can not tolerate the predicted displacements, then ground or structural remediation should be used.

It is important to recognize that the two case histories considered in this report are based on conditions whereby lateral spreading is parallel to the superstructure, which typically is one of the strong directions of the bridge. If the spreading effect is skewed with respect to the superstructure, then the skew must be accounted for in determining the likely plastic mechanism that will control.

The conclusions from this study of the effects of liquefaction when the design earthquake return period is increased from the existing AASHTO I-A 475-year return period to 2,475-years are summarized as follows.

- For both the Western and Mid-America examples there were no additional costs required to address the recommended liquefaction requirements when a bridge was designed for the current 475-year earthquake and was then subjected to the 2,475-year earthquake recommended in the LRFD provisions for the life-safety level of performance, despite significant increases in the PGA for the 2,475-year event.

- For the Western U.S. example, liquefaction occurred for the 475-year event, and it was necessary to provide stone column mitigation measures in the upper 30 feet or so. This would also most likely be necessary at both abutments (only one was studied in-depth in this effort). The cost for the stone columns at both abutments was estimated to be about 2.5 percent of the bridge cost. For the 2,475-year event similar measures were required with the depth of the stone columns extended to 50 feet. The estimated cost of this remediation is of the order of 4 percent of the bridge cost.

- For the Mid-America example, liquefaction did not occur for the 475-year event; however, the bridge was capable of meeting the liquefaction requirements for the new LRFD provisions for the 2,475-year event, with liquefaction occurring at a depth of 20 to 40 feet, through pinning action of the piles. By allowing some inelastic deformations in the piles, no ground improvement was required.

- For the Mid-America and Western U.S. sites the higher operational level of performance can be achieved in the foundation system (i.e., piles remain in their elastic capacity) for the 2,475-year event by improving the ground using stone columns. This improvement can be achieved for less than 5 percent additional cost in the case of the Western U.S. site and less than 10 percent additional cost in the case of the Mid-America site.

This study demonstrates the beneficial effects of considering the resistance that the substructure of the bridge offers to lateral movement of soil, ‘pinning’. These effects can be significant and should be considered in predictions of lateral soil movements. The study also shows the benefit of allowing inelastic behavior in the foundation under the action of lateral ground movement. For many cases relatively large displacements of the ground may be accommodated by the structure without collapse. .

There has been considerable advancement in the state of the art in assessing impacts of liquefaction since the AASHTO Division I-A provisions were developed. These have been included in the recommended LRFD provisions and used in the two case studies. They are relatively easy to use, and they permit a much better understanding of the effects of liquefaction and lateral spreading. A summary of the new enhancements is as follows:

- A better ability to estimate the displacements that may occur as a result of lateral spreading. Currently, this is not always done in liquefaction studies.

- The ability to incorporate the beneficial effects of “pinning’ of the piles and ground movement in resisting lateral flow movements.

- The new information available from USGS on the deaggregation of the ground shaking hazard into the contributions of different seismic sources, earthquake magnitude, and distances for a particular site.

- The ability to perform nonlinear stress analysis time-history studies using realistic acceleration histories of ground motion to better understand the sequence of events that occur during liquefaction and the modification in ground motions that occur as a result.

As discussed in Article A.6 there were two global options that were considered for the development of these recommended LRFD provisions. The one that was adopted was to design explicitly for a larger event (3% PE in 75 years) but refine the provisions to reduce the conservatism and gain a better understanding of what occurs in a larger event while attempting to keep the costs about the same as the current provisions. Under this scenario, the degree of protection against larger earthquakes is quantified and based on scientific principles and engineering experience. The other option which is the basis of the current AASHTO Division 1-A provisions is to design for a moderate sized event and maintain the current conservative provisions as a measure of protection against larger events. In this scenario the degree of protection is unknown and depends on intuition and engineering judgment. These examples demonstrate the benefits of the designing for and understanding what occurs in a larger event.

The implications of the new LRFD recommendations in going to a 2,475-year return period event is that there is a greater area that now requires more detailed seismic design, including a liquefaction assessment. The specific details of when liquefaction should be considered are covered in Section 3.10.5 of the provisions, but in general, liquefaction is considered for bridges classified as SDR 3 or greater for a site that has a mean magnitude earthquake from deaggregation greater than 6.4. If the mean magnitude is less than 6.0, then liquefaction is not required to be considered. Between a mean magnitude of 6.0 and 6.4, liquefaction may or may not be required to be considered depending on the combinations of soil type and acceleration levels. Although liquefaction must be assessed in certain designs, the Mid-America example has demonstrated that a bridge may meet the recommended performance requirements of the new provisions without any additional expenditure of funds. It is difficult to draw wider implications from this study without additional study.

It should be recognized that that approach recommended here for large, infrequent earthquakes is a departure from the traditional approach of preventing damage in the foundation. For ground movements on the order of those expected, it is felt that often either remediation is necessary or allowance of some inelastic action in foundation is necessary. It is recognized that only two specific examples were considered in this study, and that with time refinement will be possible as more structures are studied and designed. It is also recognized that the prediction of earthquake-induced ground movement is approximate at best, and much remains to be learned by the profession on how to produce more accurate predictions. Of all the issues, the greatest uncertainty lies in the methods of predicting ground displacements as seen in the variations of the simplified methods and the more precise nonlinear analyses. However, it is felt that the recommended approach is a reasonable beginning to rationally designing for such earthquake-induced hazards. The broader implications of these results deserves additional effort that was not part of this scope of work.